UNIVERSITÀ DEGLI STUDI DI MILANO

SCUOLA DI SPECIALIZZAZIONE IN FISICA MEDICA

FACOLTÀ DI MEDICINA E CHIRURGIA

Dosimetric feasibility study of Total Body Irradiation treatment with Volumetric Modulated Arc Therapy technique

Relatore: Prof.ssa Cristina LENARDI
Correlatore: Dott. Angelo Filippo MONTI
Correlatore: Dott.ssa Cristina DE MATTIA
Controrelatore: Dott. Roberto PELLEGRINI
Controrelatore: Dott.ssa Anna Enrica FRANCIA

<div align="right">

Tesi di Specializzazione di:
Denise Curto
Matr. S63341

</div>

Anno Accademico 2020/21

Summary

ABSTRACT

Introduction: Total Body Irradiation (TBI) is a radiotherapy treatment prescribed for patients with different form of leukaemia. It is part of conditioning regimen for hematopoietic stem cell transplantation and different techniques can be adopted to deliver TBI treatment. The conventional method consists of two static either lateral (LAT) or anterior-posterior/posterior-anterior (AP/PA) opposed photon beams, delivered with a linear accelerator (LINAC) at an extended source-surface distance, so as to cover the entire patient's body with the fields. Developments on linear accelerator and multi-leaf collimator allowed to introduce Volumetric Modulated Arc Therapy (VMAT) for TBI treatments. Different centres tried to implement this technique addressing various treatment aspects (CT simulation, planning, pre-treatment dosimetry, patient positioning and immobilization systems) and they verified its effectiveness and advantages. This thesis is a dosimetric feasibility study, which purpose is to implement VMAT-based TBI in Grande Ospedale Metropolitano (GOM) Niguarda, where TBI treatment with conventional method is currently performed.

Material & Methods: Feasibility of CT-simulation with Canon Aquilion Exceed LB CT, contouring and planning with MIM® 7.1.4 (MIM Software Inc.) and Monaco® 5.51.10 (Elekta AB, Sweden) Treatment Planning System (TPS), delivery with an Elekta LINAC equipped with Agility® (Elekta AB, Sweden) Multi Leaf Collimator (MLC) were investigated following different approaches found in literature. Dosimetric verifications of calculated and delivered doses were performed with Thermo Luminescent Dosimeters for point measurements and with the Delta^4 phantom+ (ScandiDos AB, Sweden) for 3D measurements. The human-like Alderson Rando phantom was used for the entire implementation, while two whole-body retrospective CT acquisitions of two patients undergoing conventional TBI were used for planning optimization. Treatment goals of VMAT-TBI plan were to cover almost 95% of PTV volume with 95% of prescription dose (12 Gy delivered in 6 fractions twice a day) and to reduce mean dose to lungs below 10 Gy.

Results: CT-simulation, contouring, planning and delivery of VMAT-TBI treatment were successfully performed. CT-simulation consisted of two CT-acquisitions with different orientations, one head-first supine (HFS) and the other feet-first supine (FFS). On the two CT-scans the PTV (the whole body reduced by 3 mm from the skin) and the OARs (lungs and, eventually, kidneys) were contoured, and subsequently, the planning was carried out on them. The VMAT-TBI treatment plan consisted of six overlapping fields with six different isocentres and maximum size of 40x40 cm^2. Three fields were planned on the HFS-CT, while the other three on the FFS-CT, resulting in two plans optimized thanks to Monaco "Bias Dose" tool. Dosimetry, carried out simulating the treatment on Alderson Rando with TLDs and then with Delta^4, verified that calculated dose by Monaco was comparable with delivered and measured dose. Average mean and maximum percentage differences between calculated and measured doses obtained from point measurements with TLDs were 2.3% and 10.4%. Gamma passing rate (3%/3 mm, global, 10% cut) of single beams dose distributions acquired with Delta^4 resulted always higher than 99%, while dose distributions in junction regions between adjacent fields resulted higher than 90%. VMAT-TBI simulated treatment plans of two patients fulfilled treatment goals of PTV coverage and OARs sparing: average PTV volume that receive almost 95% of prescription dose resulted 97.44%, while average mean dose to lungs was 9.89 Gy and mean dose to kidneys was 10.11 Gy.

Conclusions: This study confirms the feasibility of VMAT-based TBI in GOM Niguarda Hospital. Next step of the treatment implementation is to investigate more clinical oriented aspects, such as immobilization systems for patient's positioning and setup verifications.

CHAPTER 1

INTRODUCTION TO TOTAL BODY IRRADIATION

Total Body Irradiation is a radiotherapy treatment frequently used in conjunction with chemotherapeutic agents as a component of the conditioning regimen prior to Hematopoietic Stem Cell Transplant (HSCT) for treating several haematological malignancies[1]. The TBI irradiates the whole patient's body to eliminate the malignant cells that escape chemotherapy, to clear the host marrow to allow repopulation with donor marrow and to suppress the patient's immune system for preventing the rejection of donor bone marrow by immunologically active cells in the host[2]. There are many techniques to deliver TBI treatment and development is still in progress in order to simplify the delivery, make the treatment more comfortable to the patient, adapt it to conventional machines and rooms, decrease time of treatment, increase efficacy and reduce toxicities. This chapter deals with 1) a brief introduction to HSCT and its main characteristics, in particular the conditioning regimen, in which TBI comes into play, 2) a review on the evolution of TBI delivery techniques, focusing on the most used method currently and new developments, 3) a report on different aspects of VMAT-based TBI technique described in literature.

1.1 Hematopoietic stem cell transplant

Hematopoietic stem cells are a little fraction (0.05-0.5%) of cells in the bone marrow that are capable to generate continuously all mature cells flowing in peripheral blood. For patients with haematological malignancies or diseases involving the presence of deficient medullary function, i.e. hematopoietic stem cells do not work properly, Hematopoietic Stem Cell Transplant is established as one of the most important curative strategies, becoming an increasingly safe and effective procedure[3]. According to data summarized by the Centre for International Blood and Marrow Transplant Research, in 2005, the diseases most commonly treated with HSCT were (in decreasing order of frequency): multiple myeloma, non-Hodgkin lymphoma, acute myelogenous leukaemia, Hodgkin disease, acute lymphoid leukaemia, myelodysplastic syndrome, chronic myelogenous leukaemia, and additional malignant and non-malignant diseases[4].

Two fundamental principles underpin the development of stem cell transplantation as an effective and relatively safe clinical procedure: a combination of drugs and/or radiotherapy delivered before the infusion of stem cells, referred to as the conditioning or preparative regimen, and intravenous infusion of enough stem cells to ensure lifelong reconstitution of all hematopoietic lineages[3]. The stem cells infused in the patient during the transplant can be taken from the patient himself, we speak in this case of autologous transplantation, or from a donor in the allogeneic transplant. The choice of the type of transplant depends on different factors, like disease, patient's age and donor availability.

Alkylating agents– interfere with DNA replication by formation of covalent intercalating cross-links between DNA strands:
- busulfan*
- carmustine (BCNU)*
- cyclophosphamide[†]
- ifosfamide[†]
- melphalan*
- thiotepa*
- treosulfan*[†]

Anti-metabolites– inhibit biochemical mechanisms involved in cell division
- Fludarabine[†]

Epipodophyllotoxins – inhibit topoisomerase II during DNA replication and transcription
- Etoposide (VP-16)[†]

Platinum agents – bind with DNA, interfering with replication
- Carboplatin
- Cisplatin

Radiotherapy – direct cytotoxicity
- TBI 12–14.4 Gy*
- TBI 2–3 Gy[†]

Taxanes – inhibits dissolution of microtubules, blocking mitosis
- Paclitaxel

NB: Although most cytotoxic agents are both myelosuppressive and immunosuppressive, some are used primarily for myeloablative effect* and others predominantly for immunosuppressive effect[†].

Figure 1. Cytotoxic agents used in HSCT conditioning regimen [3].

1.1.1   Conditioning Regimens

Conditioning regimen is the procedure must be performed before transplant and it consists on a high dose chemotherapy and/or radiotherapy treatment. There are different protocols that can be adopted, involving a wide variety of cytotoxic agents. Figure 1 reports some of them with their main effect: myeloablative, immunosuppressive or both. The choice affects the intensity of the conditioning regimen and depends on disease, patient's age, previous treatment, general medical patient's conditions and degree of donor-matching. Another important factor is type of HSCT. In autologous one, there is no genetic difference between the transplanted stem cells and the patient, so the only role of the conditioning regimen is malignant cell population eradication (myeloablation). In contrast, in patients transplanted with allogeneic stem cells, a dangerous graft rejection is possible unless the host immune system is suppressed[3] (immunosuppression).

As reported in previous figure, before or after chemotherapy, also TBI can be prescribed for conditioning regimen, thanks to its unique features that make it a valuable component of transplant preparative regimens [1]:

1. no sparing of "sanctuary" sites such as testes and the central nervous system;

2. no dependence on blood supply;

3. no influence by variability in drug absorption, metabolism, biodistribution, or clearance kinetics [5];

4. less chance of cross-resistance with other antineoplastic agents (chemotherapy);

5. no problems with excretion or detoxification;

6. Ability to tailor the dose distribution by shielding specific organs or by "boosting" sites.

Regimens with TBI seem to achieve better outcomes than those without it[6–12]. Even though TBI is an efficient part of bone marrow transplantation conditioning treatment, it is responsible for many side effects associated with both acute toxicity (e.g. nausea, vomiting, diarrhea, stomatitis, temporary loss of taste, parotitis and rash) and late toxicity (e.g. interstitial pneumonitis, hepatic veno-occlusive disease, cataracts, infertility, hormone-related disorders, bone toxicity, growth retardation and secondary malignancies)[13–21]. To reduce side effects as much as possible, it is necessary to accurately select and compose complex therapeutic regimens. From the TBI perspective, improving the treatment planning methods of dose distribution, and, in consequence, methods of dose delivery to the patient could also reduce the side effects. For these reasons, TBI had been an important evolution during the years and a wide variety of fractionations and techniques have been investigated and reported in next paragraph.

1.2 Total Body Irradiation

The first use of TBI in two HSCT patients is reported by Thomas et al (1959)[22]. In this study radiotherapy was adopted for conditioning regimen because no remission of leukaemia was observed with conventional chemotherapy. The treatment dose was delivered in a single fraction and although engraftment was successful in both patients, relapse occurred within 12 weeks. During the following years, extensive experience has been accumulated with TBI given alone or concomitant to chemotherapy drugs, usually cyclophosphamide, and delivered as a single dose or fractionated. Many factors, including total dose, radiation exposure rate, fraction size, interval between fractions and use of organ shielding, have been evaluated to reduce toxicities, decrease relapse rates, and improve further the therapeutic index[23]. Numerous studies have shown that efficacy is improved and a variety of important toxicities are significantly decreased when TBI is fractionated in 2 to 3 treatments per day[24–27] (Fig. 2). Moreover, relatively low-dose rates are also important for optimal outcome[28]. Nowadays, TBI is typically given to a total dose of 10-16 Gy in 1.2- to 1.35-Gy fractions given 3 times per day or in 1.5- to 2-Gy fractions twice a day with at least 4-6 hours between fractions[5]. Moreover, a uniform dose must be delivered to the entire body with a dose homogeneity of ±10% of the prescribed dose, according to AAPM report 17[29].

Diagnosis	No. of patients	Fraction size (Gy)	No. of fractions	Total dose (Gy)	Probability of relapse	Probability of event-free survival
AML – first	27	10.0	1	10.0	0.55	0.33
remission [4]	26	2.0	6	12.0	0.20	0.54
AML – first	34	2.0	6	12.0	0.35	0.60
remission [91]	37	2.25	7	15.75	0.12	0.60
CML – chronic	57	2.0	6	12.0	0.19	0.73
phase [10]	59	2.25	7	15.75	0	0.66
Hematologic	73	10.0	1	10.0	0.37	0.38
malignancies [5]	74	1.35	11	14.85	0.23	0.45

AML, acute myeloid leukemia; CML, chronic myelogenous leukemia.

Figure 2. Randomized trials of total body irradiation regimens given with cyclophosphamide 120 mg/kg[30].
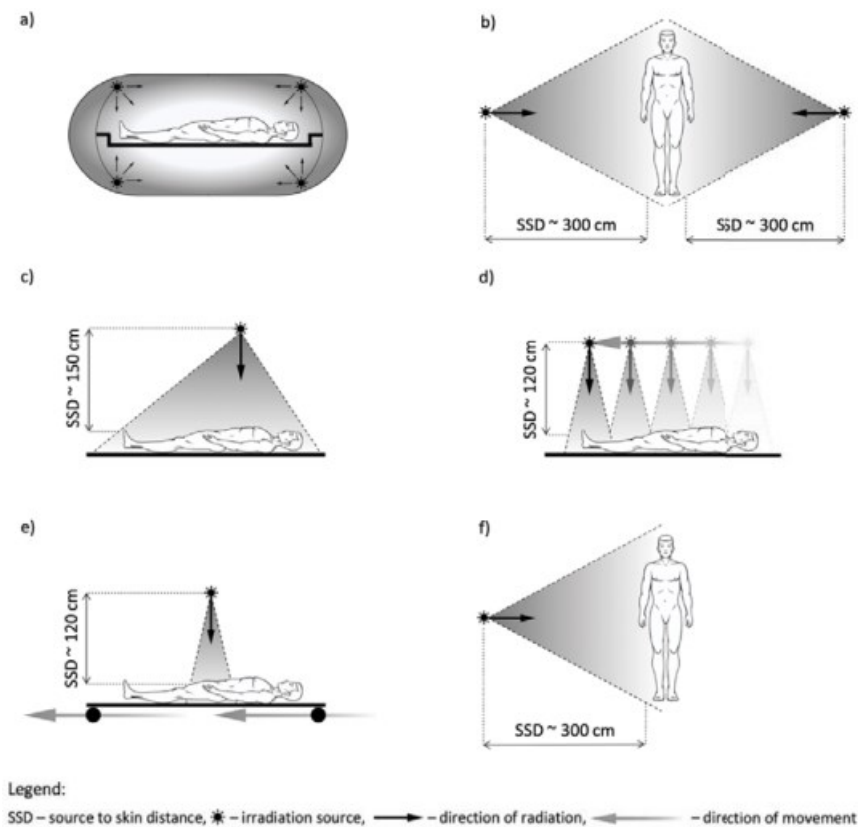
Figure 3. Historical and conventional methods of total body irradiation. The diagrams represent respectively: (a) cesium irradiation in therapeutic chamber (Jacobs and Pape[31]), (b) irradiation by two Co-60 sources (Sahler[32]), (c) irradiation on dedicated Co-60 unit (Princess Margaret Hospital, Toronto[33]), (d) irradiation by ceiling track mounted Co-60 source (Cunningham and Wright[34]), (e) irradiation by Co-60 with moving couch (Quast[35]), and (f) one of the lateral fields used for irradiation by conventional method realized with linear accelerator[36].

1.2.1 TBI delivery techniques

1.2.1.1 First approaches

For the delivery of TBI, different approaches have been adopted in the past years. Litoborska et al (2020)[36] reports a review study on evolution of treatment planning and dose delivery methods of TBI for patients undergoing HSCT. The first solution of TBI was proposed by Jacobs and Pape (1960)[31] and was based on four rods containing two Cs-137 sources in each of them. They built a TBI chamber where the sources of irradiations were separated from each other by 2 m and were placed at each end of the treatment bed (Fig. 3a). This solution was too expensive for most medical facilities and the researchers' interest was directed to the possibility of using cobalt units used in the conventional radiotherapy. In 1959, Sahler[32] developed a dual-source cobalt (Co-60) irradiator that consisted of a conventional rotating cobalt unit and an industrial large field cobalt irradiator. It allowed to arrange irradiation geometry to produce a parallel opposed field at about 3 m from the patient (Fig. 3b). The source characteristics and the distance between source and patient define this proposal as a low dose rate TBI (<0.10 Gy/min). The use of a single Co-60 source unit was introduced by investigators from the Princess Margaret Hospital in Toronto (1981)[33] (Fig. 3c), who also introduced the flattening filter to compensate the dose variation across the beam and a special lead attenuator

to obtain low dose-rate TBI. In order to diminish source-to-skin distance (SSD) Cunningham and Wright (1962)[34] realized a Co-60 unit mounted on a ceiling track, with a specially designed collimator. The source scanned the patient positioned on a therapeutic couch at about 120 cm SSD (Fig. 3d). This idea was adapted for rotating Co-60 units by Quast[35] (Fig. 3e). While in the Cunningham and Wright study, the source was moved along the long axis of the patient, Quast's solution allows the patient to be moved (through a mobile couch) beneath a fixed Co-60 source. In these techniques, lungs are the main organs at risk (OAR) and shielding strategies, like use of lead blocks, were adopted in order to reduce lungs mean dose to 8-10 Gy[36]. However, TBI delivery only at Co-60 units limited the possibility of simultaneous reduction of doses in the lungs and obtaining high doses in the chest wall, where there may be disease to be eradicated. Therefore, a combined treatment consisting of large irradiation fields on Co-60 units and the use of electron fields (on conventional linear accelerators) with energies from 6 MeV to 12 MeV (dependent on the thickness of the chest wall) was introduced to boost the chest wall region[37]. This combined treatment provided the argument to move TBI entirely from Co-60 to linear accelerators (LINACs), combining photon radiation with energies from 6 MeV to 15 MeV[38–42] and electrons.

1.2.1.2 Recent techniques and conventional method

In 2014, Giebel et al[43] published a survey of the Acute Leukemia Working Party of the European Group for Blood and Marrow Transplantation in which they investigated different myeloablative TBI techniques used in clinical practice. 56 centres, located in 23 countries (19 European countries), answer to the survey, which consists in a questionnaire regarding different aspects of TBI methodology. Table 1 shows different parameters of TBI reported in the survey, the most frequent according to the survey and those adopted in our centre, GOM Niguarda Hospital. 11 different techniques were found to be used, but the most prevalent method (64% of centres) for delivering TBI is "patient in 1 field". This is the one that is currently used in GOM Niguarda Hospital and in this thesis will be referred as the "conventional" method (cTBI). It consists of two stationary opposed high energy photon beams in anterior-posterior or lateral direction with the largest possible field size (Fig. 3f). The patient typically stands on a stand designed for TBI delivery (Fig. 4A) or lies on a gurney (Fig. 4B) at an extended SSD (3-4 m), which allows to reduce the dose rate to about 10% compared to SSD distance. The collimator of the treatment field is rotated by 45° to use the diagonal dimension of the field and irradiate the entire length of the patient in one radiation beam. Often the treatment room height is not suitable for geometries required by TBI, so the gantry is rotated by 90° so as to take advantage of the width of the room. Lead blocks, designed from radiographs obtained while the patient is in the standing treatment position, cover the central portion of the lung, with approximately 1 or 2 cm between the edge of the lung shadow on the film and the edge of the block[5] (Fig. 5). Moreover, it should be noted that for certain types of TBI-treated diseases, like leukaemia, it is preferred that the skin receive a full dose of radiation. Therefore, to defeat the skin-sparing effect related to build-up condition of high-energy photons, a beam spoiler of low atomic number material, such as PMMA is placed close to the patient[44]. This large field radiotherapy technique can be implemented in different ways, depending on equipment available and selecting physical parameters that should be considered and optimized for each individual institution. The most common options relate to a) the energy of radiation, b) treatment distance, c) choice of antero-posterior (AP) treatments, lateral treatments or a combination of these, and d) dose rate.

Parameter	Giebel et al survey[43]	Most frequent[43]	GOM Niguarda Hospital
Prescription	8-14.4 Gy	12 Gy (64%)	12 Gy
Number of fractions	1-8	6 (64%)	6
Dose/fraction	1.65-8 Gy	2 Gy (64%)	2 Gy
Dose rate	0.0225-0.375 Gy/min	0.16 Gy/min (6.5%)	0.07 Gy/min
Treatment unit	LINAC or Cobalt unit	LINAC (91.1%)	LINAC
Photon energy	6-25 MV	6 MV (51%)	15 MV
SSD	2-5 m	4 m (18%)	4 m
Techniques	Patient in 1 field Multiple isocentres Moving strips Segmented fields SSD (3 parts) Sweeping beam Moving couch Patient in multiple fields	Patient in 1 field (64.3%)	Patient in 1 field
Dose to lungs	6-14.4 Gy	8 Gy (21.4%)	9 Gy

Table 1. Parameters of TBI treatment reported in the Giebel et al's survey, used most frequent according to the survey and parameters adopted in GOM Niguarda Hospital.
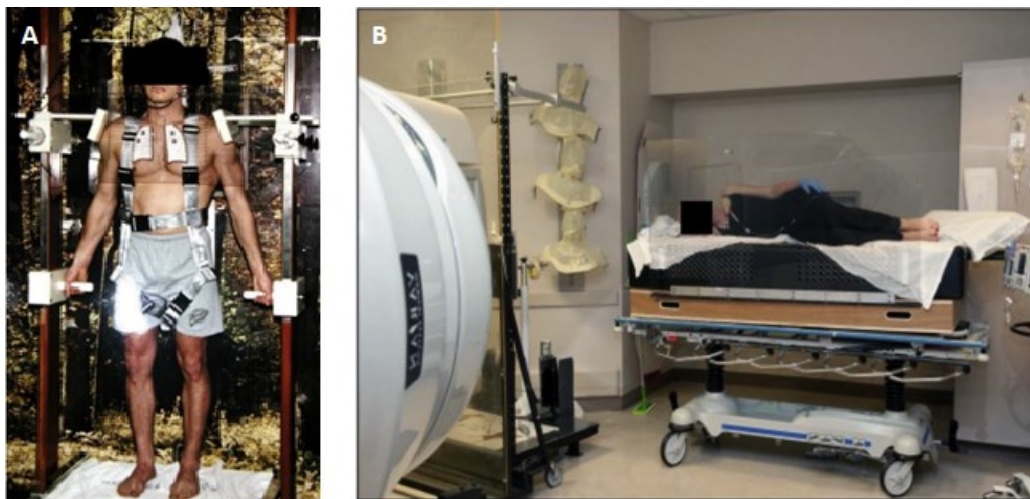

Figure 4. Two setups for receiving total body irradiation (TBI) with conventional method. In both cases, the patient's position is reversed for posteroanterior (PA) treatment[5].
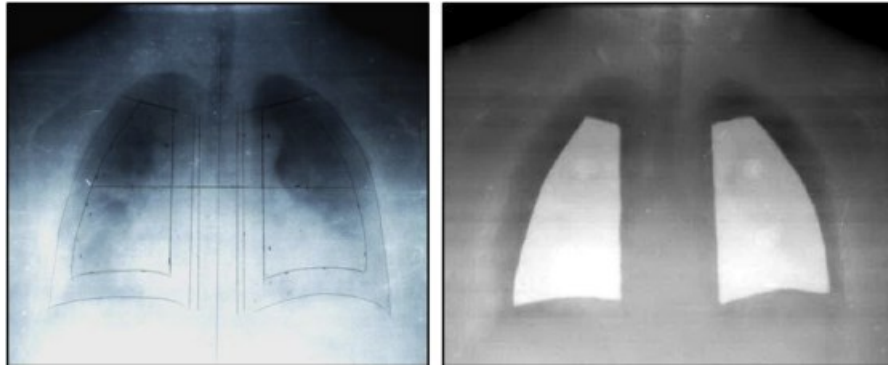
Figure 5. Lung blocks from planar images in the standing position. Typical margins used are 2 cm from the diaphragm and vertebral edge, 1.5 cm from the rib cage and at the bottom edge of the clavicle. Lung blocks can be modified depending on the clinical circumstances. (Left) A chest x-ray image used for block design. (Right) A portal image obtained with LINAC radiation during treatment delivery for verification of block placement[5].

In particular, in our centre, photon energy is 15 MV, dose rate is about 0.07 Gy/min in the axis of the beam, gantry of the LINAC is rotated by 90° and collimator by 45°, SSD is equal to 4 m, patient lies on a gurney as in Fig. 4B, lungs are shielded with lead blocks attached to a compensator hooked to the gantry and their position is verified at each fraction with a Computed Radiography (CR) system and a beam spoiler of 3 cm-PMMA material is positioned close to the patient. 12 Gy, prescribed at the patient's midplane at the level of navel, are delivered in 6 fractions twice a day.

The planning procedures for the cTBI method based on geometrical measurements and simplified calculations of doses are controlled by in-vivo measurements[45]. Guidelines for dosimetry are reported by AAPM TG. 17[29] and different type of detectors can be used, including semiconductors, thermoluminescent dosimeters (TLD), metal oxide semiconductor field effect transistor (MOSFET), ionization chambers and alanine dosimeters[43]. Currently at GOM Niguarda Hospital, in-vivo dosimetry is performed with six diodes: three on the entrance surface and three on the exit surface of the patient. They are positioned at three reference patient's height: on forehead, on one of the two lungs and on lower abdomen. Diodes provides point measurements and doses at patient's midplane for the three positions are evaluated averaging entrance and exit doses. Diodes allows to obtain instant measurements, so that dose can be verified on-time and MU needed to deliver prescription dose can be adjusted on-line. The accepted discrepancy between the planned, 12 Gy to the total body and 9 Gy to the lungs delivered in 6 fractions, and measured doses is within 5%.

1.2.1.3 Modern methods

The TBI methods described so far rely on point measurements that are a big simplification of the full dose distribution, which can result in larger-than-expected heterogeneity in organs at risk and target structures. Hui et al[46] used computed tomography (CT)-based three-dimensional (3D) planning to analyse dose distribution in patients receiving TBI with lateral beams and demonstrated that conventional planning methods resulted in larger-than-expected dose variations throughout the body, with some portions of the lung receiving up to 32% above the prescribed dose. Increasing
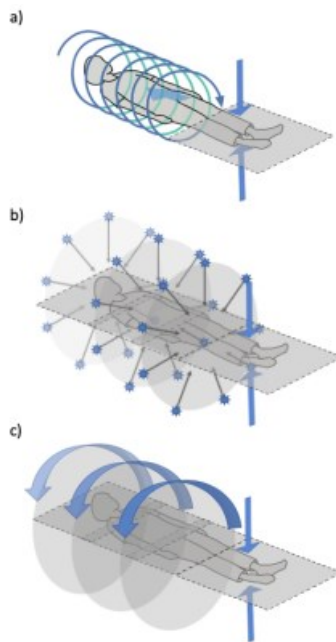
Figure 6. Current solutions of TBI. The graphs represent respectively: (a) irradiation realized on Tomotherapy machine, (b) irradiation realized through three plans, each plan containing nine equispaced intensity-modulated photon beams, and (c) irradiation realized through three plans, each plan containing three volumetric modulated photon arcs. In each method, two opposite photon beams are used for the irradiation of the area from the middle part of the femur to the toes[36].

development of CT-based 3D planning, intensity-modulated radiation therapy (IMRT), inverse planning and advanced calculation algorithms allowed to improve dose uniformity and sparing of organs, also different than lungs. Among the new equipment, Tomotherapy (Fig. 6a) revolutionized the concept of preparing and performing the TBI procedure thanks to the possibility of preparing a treatment plan including the optimization of dose distribution on CT images and image guidance procedures[47,48]. However, the relatively long beam-on time they took (more than 30 min) was pointed as a potential problem of stability during dose delivery. Parallel to the development of TBI on Tomotherapy, its implementation with Intensity-Modulated Radiation Therapy (IMRT) realized through large fields on conventional linear accelerators was discussed[49,50] (Fig. 6b). Advantages to this approach include the ability to treat patients while they are supine, which is both more comfortable and more reproducible than position of conventional treatment, as well as the ability to conduct CT-based simulation and image-guided radiotherapy. Last developments on LINACs and Multi-Leaf Collimators (MLC) allowed to introduce also Volumetric Modulated Arc Therapy (VMAT) for TBI (Fig. 6c). In the lasts 10 years, different centres in Europe, America and Asia tried to implement this technique and some studies about first experiences can be found in literature. In 2015, Chakraborty et al[51] presented a feasibility study of VMAT-TBI implemented with the Treatment Planning System (TPS) Eclipse™ and RapidArc™ LINAC by Varian. A first clinical experience of 7 patients treated between 2013 and 2014 is reported by Springer et al[52] (2016), which describes also dosimetric checks with ArcCheck phantom and in-vivo dosimetry with MOSFETs. Symons et al[53] (2017) implemented VMAT-TBI using Pinnacle[3] TPS and Elekta Agility™ LINAC, while Tas et al[54] (2018) used Versa HD™ with Agility® collimator system and Monaco 5.11® TPS (Elekta AB, Sweden) and Uehara et al[55] (2021) used Halcyon™ LINAC and Eclipse™ TPS. A novel

rotatable tabletop in order to simplify patient positioning was proposed by Ouyang et al[56] (2017), Losert et al[57] (2019) and Zhang-Velten et al[58] (2021). Guo et al[59] (2021) implemented a robust planning technique with image-guided delivery to improve dose delivery accuracy and a streamlined sim-to-treat workflow with automatic scripts to reduce planning time.

1.2.2 VMAT-based TBI

This section reports a review about different aspects of the VMAT-based TBI treatment, as CT-simulation, contouring, planning and dosimetry checks, found from literature and studies cited previously. These aspects are summarized also in the following table (Table 2).

Study	*Chakraborty et al (2015)[51] Malabar cancer centre, India*	*Springer et al (2016)[52] Elisabethinen Hospital Linz, Austria*	*Tas et al (2018)[54] Yeni Yuzyil University Gaziosmanpasa Hospital, Istanbul, Turkey*	*Zhang-Velten et al (2022)[58] University of Texas, Southwestern Medical Center*	*Losert et al (2019)[57] Department of Radiation Oncology, University Hospital, Munich, Germany*	*Uehara et al (2021)[55] Kindai University, Osaka, Japan*	*Symons et al (2017)[53] Genesis Cancer Care WA, Fiona Stanley Hospital, Australia*
CT-scan	HFS	HFS+FFS Thickness of 5 mm	HFS+FFS	HFS+FFS 10 cm overlapping; Thickness of 5 mm	HFS+FFS Thickness of 5 mm	162 cm whole-body CT	HFS+FFS Thickness of 5 mm
Immobilization system	Not described	Vacuum mattress and thermoplastic mask for head and shoulders	Vacuum mattress and thermoplastic mask for head	Rotational body frame with Vac-Lok bag	Rotatable tabletop with different immobilization devices for head and thorax (HeadSTEP and iCAST systems), abdomen and legs (ProSTEP system) and arms (indexed bars)	Not described	Thermoplastic mask for head and neck region, and vacuum bag
PTV contouring	Whole body contracted of 3mm from skin	Whole body without OARs	Whole body contracted of 3mm from skin and into OARs	Whole body contracted of 5 mm from skin and into lungs	Whole body contracted of 5mm from skin and into lungs	Whole body contracted of 3mm from skin	Whole body contracted of 5mm from skin and 3 mm into lungs
OARs contouring	Lungs and kidneys	Lungs and eventually kidneys or brain	Lungs, kidneys and lens	Lungs, spinal cord, bowel, kidneys, oral cavity and whole brain	lungs	Lungs, lens, kidneys, testes	Lungs, kidneys and liver
prescription	12 Gy in 10 fractions to 95% of PTV	13.2 Gy in 8 fractions twice daily; 10 Gy to lungs	12 Gy in 6 fractions twice a day to 90% of PTV; D_{mean}<10 Gy to lungs	12 Gy in 8 fractions twice a day	10-12 Gy; 8-10 Gy to lungs	12 Gy in 6 fractions to 50% of PTV; D_{mean} <10 Gy to lungs and kidneys; D_{mean} <9 Gy to lens; D_{mean} <5 Gy to testes	12 Gy in 6 fractions to 90% of PTV; D_{mean} <8 Gy to lungs; D_{mean} <9 Gy to kidneys and liver

Study	Chakraborty et al (2015)[51] Malabar cancer centre, India	Springer et al (2016)[52] Elisabethinen Hospital Linz, Austria	Tas et al (2018)[54] Yeni Yuzyil University Gaziosmanpasa Hospital, Istanbul, Turkey	Zhang-Velten et al (2022)[58] University of Texas, Southwestern Medical Center	Losert et al (2019)[57] Department of Radiation Oncology, University Hospital, Munich, Germany	Uehara et al (2021)[55] Kindai University, Osaka, Japan	Symons et al (2017)[53] Genesis Cancer Care WA, Fiona Stanley Hospital, Australia
LINAC	RapidArc (Varian Medical System)	RapidArc (Varian Medical System)	VersaHD with Agility MLC (Elekta AB, Sweden)	TrueBeam and VitalBeam with millennium MLC (Varian Medical System)	Axesse with Agility MLC (Elekta AB, Sweden)	Halcyon™ (Varian Medical System)	Agility (Elekta AB, Sweden)
Treatment Planning System	Eclipse 10.0 (Varian Medical System)	Eclipse (Varian Medical System)	Monaco 5.11 (Elekta AB, Sweden)	Eclipse (Varian Medical System)	Monaco 5.11 (Elekta AB, Sweden)	Eclipse 15.6 (Varian Medical System)	Pinnacle³ SmartEnterprise 9.10 (Philips Healthcare)
Photon energy	6 MV	6 MV	6 MV	10 MV for VMAT beams; 6 MV for AP-PA beams	6 MV	6 MV FFF	6 MV
Dose rate	200 MU/min	Not specified	Mean=250 MU/min (50-600 MU/min)	40 MU/min for VMAT beams and 600 MU/min for AP-PA beams	Not specified	Max=600 MU/min	No restrictions
Fields	3 VMAT isocentres; Field size=15x40	9-15 isocentres depending on body mass index; Field size=30x40; Overlap=2 cm	3 VMAT isocentres for HFS and 1-2 for FFS; Field size=40x40; Beams overlap=2 cm	3-4 VMAT isocentres for HFS and 2-3 AP-PA beams for FFS	4 VMAT isocentres for HFS and 2 for FFS	13 isocentres; Field size=28x28; Overlap=2 cm	4 VMAT isocentres (9 arcs) for HFS; Field size=18x40; Beams overlap= 4 cm; AP-PA beams for FFS
Setup verification	Not described	OBI-kV imaging system for every isocentres	CBCT for every isocentres and laser-based optical surface-guided system for intra-fraction movements	CBCT chest isocentre	CBCT of some isocentres and optical surface scan at first fraction. Room-laser system for other fractions	Not described	Not described
Dosimetry	Octavius II	• ArcCHECK for pre-treatment dosimetry • MOSFET for in-vivo dosimetry	DVH-based 3D patient dose verification composed by Dolphin® detector and Compass® software	Point measurments in solid water Radiocromic films	Not described	ArcCHECK, EPID and pinpoint ionization chamber	ArcCHECK

Table 2. Parameters of VMAT-based TBI reported in literature. HFS = Head First Supine CT-scan; FFS = Feet First Supine CT-scan; PTV = Plannning Target Volume; OAR = Organ at Risk.

1.2.2.1 Simulation and positioning

The first phase of a radiotherapy treatment is the simulation on Computed Tomography (CT) scan. For VMAT-based TBI treatment, a total body CT acquisition is required to accomplish treatment of the whole-body length. This necessity involves some critical issues. The first one is caused by limitations in the CT scan length and couch movement in most Computed Tomography models, which implies that it is not possible to acquire the entire patient's body in a single head-first supine position. The second one is the large number of images acquired for a total body scan, that could overload the archive. To overcome these problems, different centres suggest performing two CT acquisitions, one in head-first supine (HFS-CT) position from head vertex to femurs and the other in feet-first supine (FFS-CT) position from feet to pelvis, and reconstruct them with 3 mm, 5 mm or 10 mm slice thickness. The two acquisitions must overlap at least 10 cm to facilitate image fusion. This method is required usually for patients taller than 100-120 cm, depending on maximum CT scan length. For shorter patients, a unique scan is suggested.

During the simulation phase, best patient's positioning and immobilization systems are chosen: the patient should be positioned for treatment in the same way as he was positioned during the simulation. The most adopted immobilization systems in literature are thermoplastic masks, that is used to immobilize head or also shoulders, and vacuum mattress, that can take form of the body. The main critical issue is due to patient's repositioning between head-first scan and feet-first scan, in fact he must get out of couch and turn, positioning himself with his feet on head-side. For this reason, some centres[56,58,60] develop dedicated rotational immobilization systems that avoid the need to reposition the patient between two scans. They consist of a board with a support that attaches to the CT scan and LINAC couches and allows rotation, inserts to immobilize the head, legs and feet, and handles to position the arms always in the same way.

1.2.2.2 Contouring

In diseases for which TBI is prescribed, target cells are widely distributed throughout the entire body, therefore the target volume is whole body including the entire bone marrow. In particular, Planning Target Volume (PTV) is defined 3-5 millimetres below skin (body contouring), in order to achieve electronic equilibrium inside target. With regard to organs at risk, it is necessary to consider that the resulting doses obtained from TBI treatment to organs such as eyes, heart, liver, kidneys, and lungs can cause significant acute and chronic toxicities. These toxicities include cataract[28,61–65], growth retardation in children[66–68] and pneumonitis[14,15,17–19,69–71]. Furthermore, TBI has been linked with increased risk of secondary cancers of the skin, thyroid, brain, and central nervous system[20,21,72,73]. Being pneumonitis the most significant risk, lungs are always contoured as organ at risk, but in some studies also lens and kidneys are identified. One of the most advantage of VMAT-based TBI is the possibility to contour, even at a later time, all organs in order to know doses that such organs have absorbed due to the treatment. In this way, if there is the necessity to boost some organs or the patient will undergo another radiotherapy treatment, clinician has information about doses to prescribe or constraints to be respected.

1.2.2.3 Planning

Prescription dose depends on the protocol that is adopted by the centre, but in general it is equal to prescription of conventional method, i.e. 12-13.2 Gy in 6-8 fractions spread over 3-4 days. Being radiation induced pneumonitis the most significant toxicities, lungs are considered as the dose-limiting factor in TBI treatments. It has been shown that lethal pulmonary toxicity (LPC) is correlated to the mean lung dose: 6-month LPC risk is reported to be about five times higher in patients with mean lung dose greater than 9.4 Gy[19]. To eliminate this risk, lead blocks shielding lungs are used in conventional method, but for VMAT-based TBI they are not necessary. Inverse planning allows to limit OAR dose thanks to the use of constraints. So dose to lungs, and eventually kidneys, is limited to be lower than 10 Gy, while dose to lens, when they are contoured, is limited to 6 Gy.

To irradiate the whole patient's body, the plan consists of 3-4 isocentres planned on the HFS-CT (one for the head, one for the chest, one or two for abdomen and pelvis) and 2-3 isocentres planned on the FFS-CT (Fig. 7). Some centres decide to plan all isocentres with VMAT technique, while others choose to irradiate the inferior part (legs) with two AP-PA beams. The size of the fields is chosen as the maximum possible by almost all centres in order to decrease number of isocentres and accordingly time of treatment. To ensure dose homogeneity all centres choose to use overlapping fields and the junction regions between adjacent fields size from 2 cm to 5 cm (see table 2). Photon energy usually used is 6 MV. Other calculation parameters depend on TPS and type of LINAC that are used.
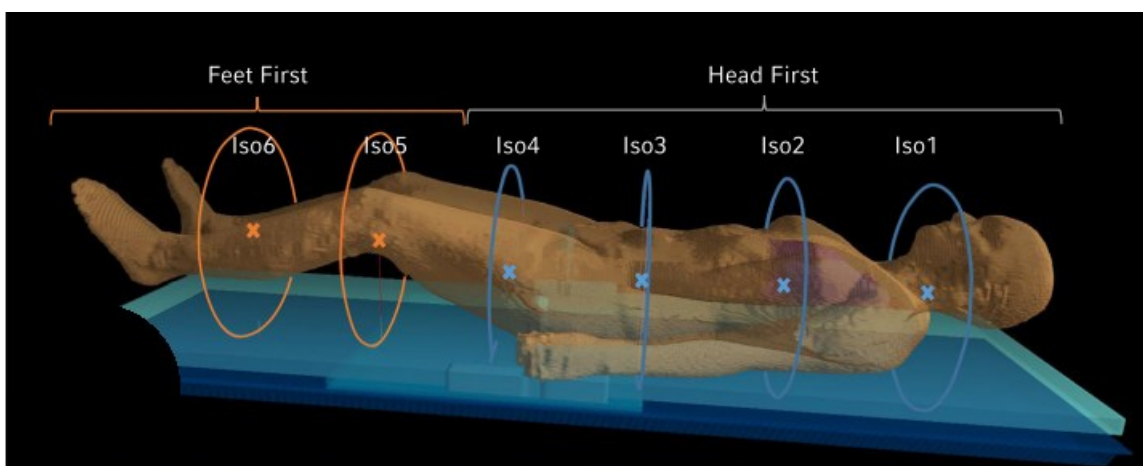
Figure 7. Isocentres planned in VMAT-based TBI[57].

1.2.2.4 Patient setup verification

The use of beams with different isocentres that overlap each other presents critical issues that must be managed correctly. In order to assure correct beam overlaps and no risk of hot/cold-spots due to incorrect patient's positioning, all centres adopt Image-Guided Radio Therapy (IGRT) thanks to Cone-Beam CT (CBCT). CBCT is performed for every isocentre before beam delivery and patient's position is adjusted if it is necessary. Moreover, some centres suggest also the use of laser-based optical surface-guided devices, like Sentinel® or Catalyst® (C-RAD AB, Sweden), for intra-fraction motion detection.

1.2.2.5 Dosimetric verifications

In literature, different instruments of measurement are adopted for VMAT-based TBI pre-treatment dosimetry: 3D ionization chamber/diode array phantoms, like ArcCHECK® (SunNuclear)[52,53,55], 2D array phantoms, like Octavius II (PTW)[51], electronic portal imaging device (EPID)[55], Gafchromic films[58], ionization chambers, ThermoLuminescent Dosimeters (TLD)[2] and metal-oxide-semiconductor field-effect transistors (MOSFET)[52]. Critical issue in this phase is verification of dose distribution in junctions between fields. These can be verified using a humanlike phantom, as proposed by Surucu et al[2], that performed point dose measurements with TLD placed inside Rando phantom. Another method is proposed by Morrison et al[74] who managed to arrange the ArcCHECK® phantom in order to measure the dose distribution in the junctions.

Study	PTV D$_{mean}$ (Gy)	PTV D$_{98\%}$	PTV D$_{2\%}$	Lungs D$_{mean}$ (Gy)	Kidneys D$_{mean}$ (Gy)
Tas et al (2018)[54] Yeni Yuzyil University Gaziosmanpasa Hospital, Istanbul, Turkey	12.7±0.1	-	-	9.7±0.2	9.6±0.2
Ouyang et al (2017)[56] University of Texas, Southwestern Medical Center	12.8±0.6	-	-	7.9±0.5	-
Chakraborty et al (2015)[51] Malabar cancer centre, India	12.00	11.33	12.52	8.65	9.86
Uehara et al (2021)[55] Kindai University, Osaka, Japan	12.6	8.9	14.2	9.6	8.5
Symons et al (2017)[53] Genesis Cancer Care WA, Fiona Stanley Hospital, Australia	12.7	-	-	7.6	6.9

Table 3. Planning outcomes for PTV and OARs achieved in different centres.

1.2.2.6 Treatment outcomes and toxicities

Table 3 reports planning outcomes from different centres. In particular, Ouyang et al compare dose distribution and dose-volume histogram (DVH) of VMAT-based TBI with a simulated plan of conventional method (Fig. 8). They found an increase in the dose in the PTV (D$_{mean}$=12.8±0.6 Gy vs. 11.5±0.2 Gy, p<0.001) and a decrease in the dose in the lungs (D$_{mean}$=7.9±0.5 Gy vs. 8.8±0.2 Gy, p<0.001)[56].

Another parameter that can be analysed as outcome is treatment time. In literature there are conflicting opinions. In some studies, VMAT-based TBI takes less time for delivery, because setup verification and corrections are easier than cTBI, even if it is based on multiple isocentres and

accordingly more movements and verifications. However, VMAT treatment requires long time for contouring, dose calculation and optimization. Table 4 reports treatment time taken in various centres. The big differences observed are due to the strong dependence on implementation of the technique (TPS, LINAC, immobilization systems, setup verifications, dosimetry) that is implemented in each centre, but some of these found an overall time comparable to cTBI[56,58].

Lastly, regarding results on patients (survival, relapse and toxicities), a study by Zhang-Velten at al[58] reports treatments outcomes from a six-year clinical experience using VMAT technique for TBI on 32 patients. They found that survival outcomes in their cohort of VMAT-TBI patients were as expected and similar to prior studies[75–78]: 1- and 2-year Overall Survival (OS) were 90% and 79%, respectively; 1- and 2- year Relapse-Free Survival (RFS) were 88% and 71%, respectively. The most common noted acute toxicities—fatigue, mucositis, and diarrhea—were all expected low-grade toxicities that are common with most conditioning regimens for HSCT and likely multifactorial in cause. Statistics of acute toxicities encountered after VMAT-based TBI treatment is reported by Tas et al[54] (Fig. 9). The dose-limiting toxicity, grade 3+ pneumonitis, believed to be directly related to TBI, had an incidence of 12.5%, comparable to conventional TBI, in which grade 3+ pneumonitis can occur in 10% to 30% of patients even with the use of lung shielding and fractionation[69,79,80].
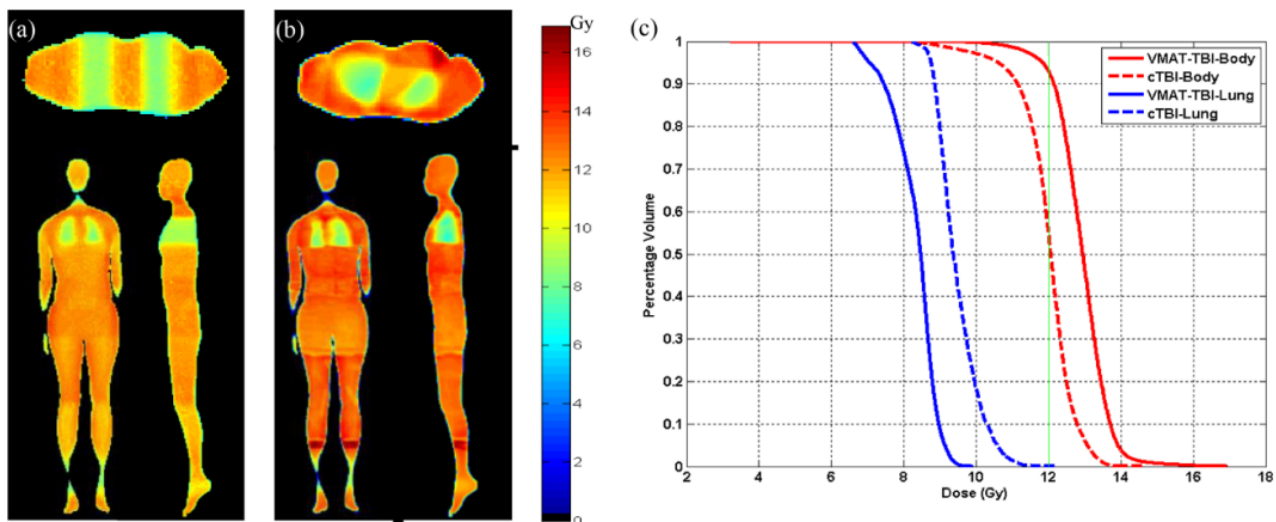

Figure 8. Three cross-sectional views of dose distribution in a sample patient with (a) cTBI; (b) VMAT-based TBI, with the dose scale illustrated by the color bar. (c) The DVHs of PTV-body (red) and lung (blue) for VMAT-based TBI (solid lines) and cTBI (dashed lines)[56].

Study	Contouring time	Optimization time	Delivery time	Quality assurance time
Springer et al (2016) Elisabethinen Hospital Linz, Austria	5-6 h	25-30 h	1.5-2 h	6-8 h
Tas et al (2018) Yeni Yuzyil University Gaziosmanpasa Hospital, Istanbul, Turkey	-	-	35-55±5 min	-
Zhang-Velten et al (2022) University of Texas, Southwestern Medical Center	-	-	72.2 min (33-147 min)	-
Losert et al (2019) Department of Radiation Oncology, University Hospital, Munich, Germany	-	-	38-57 min	-
Uehara et al (2021) Kindai University, Osaka, Japan	1-2 h	3-4 h	23 min (beam-on time)	2-3 h
Symons et al (2017) Genesis Cancer Care WA, Fiona Stanley Hospital, Australia	-	21 h	1-1.5 h	6-8 h

Table 4. Treatment time taken for different aspects during implementation of VMAT-based TBI in various centres.

Grade 1 and 2 acute toxicity	Number of patients (%)
Patchy mucositis	16 (62)
Fatigue	9 (35)
Loss of appetite	6 (23)
Xerostomia	7 (27)
Faint or dull erythema	4 (15)
Nausea not requiring antiemetics	12 (46)
Headache	11 (42)
Neck pain	8 (31)

Figure 9. Acute radiation morbidity encountered by Tas et al[54].

CHAPTER 2
MATERIAL AND METHODS

In this chapter, material and methods used to conduct the dosimetric feasibility study for implementation of VMAT-based TBI in GOM Niguarda Hospital are described. The VMAT technique wants to be introduced for TBI in our centre because in the last 5 years number of patients to be treated increased significantly as reported in table 5, and its potential advantages may benefit and facilitate the treatment. The principal advantage is the easier and more comfortable positioning of the patient, in addition to the possibility of position verifications without external systems, as Computed Radiography, but using Cone Beam Computed Tomography (CBCT), almost integrated in all accelerators. Moreover, VMAT technique allows to create patient personalized treatment plans: clinicians have information about dose distributions in target and organs at risk (identified on CT-scans acquired during treatment simulation) that allows them to make targeted prescriptions for the individual patient.

Feasibility of whole-body CT-scan, planning and optimization with Monaco TPS (Elekta AB, Sweden), delivery with an Elekta LINAC equipped with Agility MLC and dosimetry were investigated following suggestions and indications from literature reported in the previous chapter. A human like phantom was used for the entire implementation, as well as TLDs and a diodes array phantom for dosimetry.

Year	N. patients
2021	18
2020	10
2019	4
2018	4
2017	3

Table 5. Number of patients treated with TBI in last 5 years at GOM Niguarda Hospital.

2.1 Alderson Rando phantom

Alderson Rando is a humanlike phantom representing a standard patient from head to thighs. It consists of 2.5 cm thick transversal slices of tissue-equivalent material that contains bones and inserts to simulate lungs. Each slice has holes which are plugged with bone-equivalent, soft-tissue or lung tissue-equivalent pins which could be replaced by TLD holder pins for dosimetry. Figure 10 shows an Alderson Rando with numbering of slices, from 1 to 34.
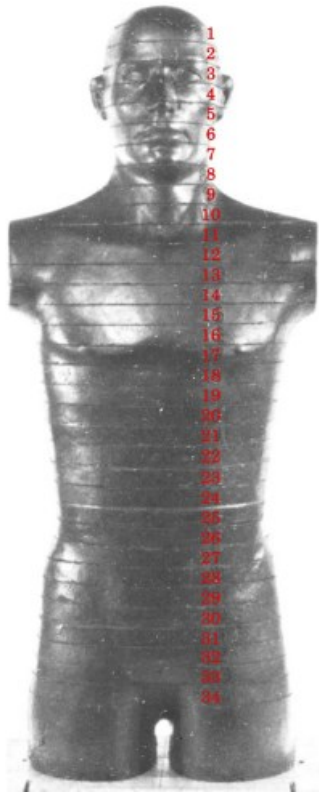
Figure 10. Alderson Rando phantom with numbering of slices.

2.2 CT simulation

VMAT-TBI treatment simulation was performed with Canon Aquilion Exceed LB CT and the first step was to understand if it was possible to acquire a whole-body scan. According to technical characteristics of the CT system used, maximum scan length is about 180 cm, so whole-body acquisition is theoretically possible for patients up to 180 cm tall. However, due to couch limitations (the couch is the same of that is installed in treatment room), the maximum length that can be acquired in a single scan has been verified of about 160 cm. In order to verify CT-scan feasibility, Alderson Rando was used. Being the phantom tall about 100 cm only, two legs were simulated with bottles of water, reaching a total height of about 180 cm (Fig. 11). Acquisition of the whole phantom was performed with two scans: one in head-first supine position (HFS-CT) and the second in feet-first supine position (FFS-CT). The first scan length was of 110 cm, the second one was of 90 cm. The two acquisitions had a slice thickness of 5 mm and an overlap by about 30 cm, so that image fusion is easier. To ensure phantom alignment in two scans, and subsequently for treatment delivery, the Alderson Rando was signed with appropriate markers for correct repositioning with respect to lasers of the CT/LINAC.

The Canon Aquilion Exceed LB CT has possibility to perform acquisition with current modulation. This is not important for acquisition of the phantom, but it allows to optimize dose to patients. Once the acquisition protocols were set with the Alderson Rando, a whole-body CT scan of a patient, underwent cTBI treatment, was performed in order to optimize planning on a real patient.

Figure 11. CT acquisition of Alderson Rando phantom with legs made of bottles of water in order to reach 180 cm height.

2.3 Contouring

In HFS-CT acquisition of Alderson Rando, the phantom whole-body, the left and right lungs were contoured using Monaco 5.51.10® (Elekta AB, Sweden) TPS. In particular, "Threshold" and "EZ Sketch" tools provided automated contouring. Thanks to "Margins" tool, a PTV was created contracting by 3 mm whole-body and lungs contours. In FFS-CT acquisition body and PTV were contoured to investigate planning feasibility with Monaco TPS. In the real patient CT acquisitions, also left and right kidneys were contoured (Fig. 12).

During planning phase, a problem due to segmentation with Monaco was encountered. The TPS is not able to manage an external contour which is not completely joined in transversal CT-slices and a large target. It is the case of legs or arms if they are not positioned tight to each other or to the body. To overcome this issue, another external contour with almost 3 cm margin from patient's body contour was drawn. In the thesis, "external" will refer to this last contour, while "patient" to the contour of the body.

Another software that can be used for contouring is MIM® 7.1.4 (MIM Software Inc.), that also allows image fusion thanks to a "Stitcher" tool (MIM software plug-in), creating two whole-body CT-images with two different orientations: one head-first and the other feet-first. Contours can be drawn with Whole Body (for patient contour) and Region Grow (lungs and kidneys) tools. Then, CT and structures can be exported on Monaco for planning. This method is preferred due to faster contouring and easier manage and visibility of PTV contour and fields in whole-body scans.
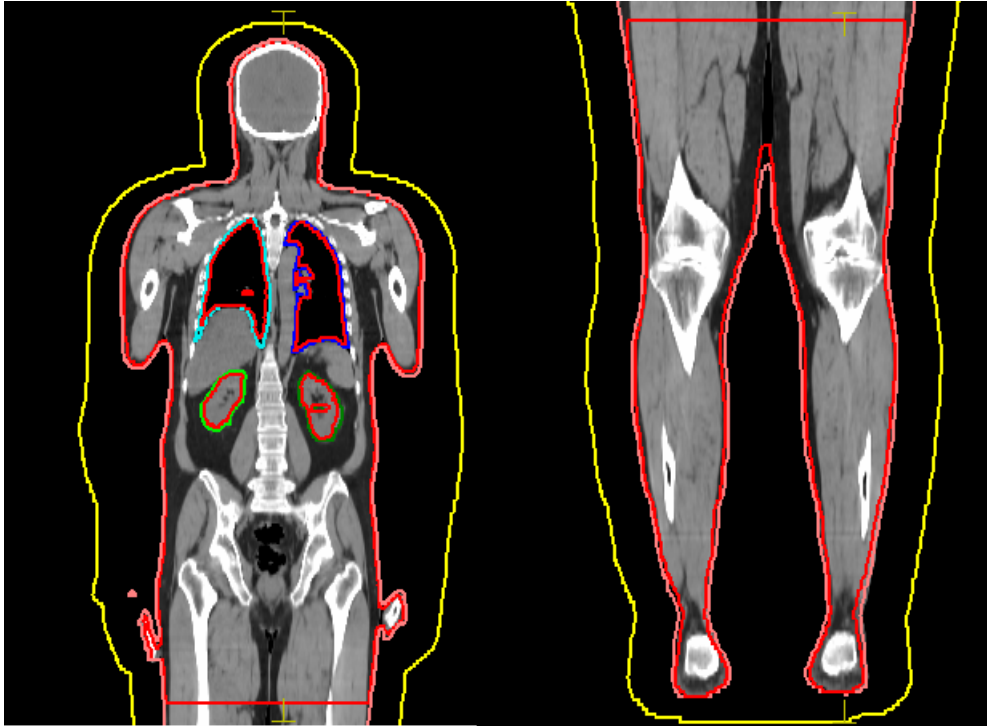
Figure 12. Patient's contouring in HFS-CT (left) and FFS-CT (right). External (yellow), patient (brown), right and left lungs (light and dark blue respectively), right and left kidneys (light and dark green respectively) and PTV (red) contours are shown. PTV was obtained contracting by 3 mm patient, lungs and kidneys contours.

2.4 Treatment planning

TBI was implemented using Elekta linear accelerator with Agility® (Elekta AB, Sweden) collimator system. This collimator system included 160-leaf MLC, minimum leaf width being 5 mm, and maximum field size 40x40 cm^2 at nominal SAD at 100 cm. VMAT plans were generated on Monaco® TPS. Monaco has the XVMC Monte Carlo dose engine, for electron and photon, for continuous arc calculation as a single beam, rather than just dose approximations that occur with many discrete (control point) gantry angle positions. Calculation parameters were grid spacing 0.5 cm, minimum segment width 1.0 cm, maximum 300 control points per arc, fluence-smoothing medium, statistical uncertainty 2.0% per calculation, gantry increment of 30°, and calculate dose deposition to medium. The VMAT-TBI technique consisted of five or six, depending on patient's height, isocentres spaced 36 cm apart and an equal number of dual-arc overlapping fields. Being the maximum longitudinal dimension of the fields equal to 40 cm, overlapping fields had junction regions (between adjacent fields) sizes up to 4 cm, following indications of Elekta case study by Bhatt et al (2021)[81] that worked with Elekta TPS and LINAC. Another study by Tas et al (2017)[82] verified that dual-arc VMAT technique (MLC mostly move just one side of the field in first arc of VMAT and then MLC mostly move other side of the field in second arc of VMAT) decreases MUs and delivery time of treatment respect to single arc VMAT technique, and moreover, a benefit can be demonstrated with regard to dose distribution and homogeneity and dose-reduction to organs at risk. In our case, for the planning on CT acquisition of the real patient, six isocentres and fields were used to cover the entire patient's height. Three fields were planned on HFS-CT scan, the other three were planned on FFS-CT. Because of the limited couch motion capacity of the LINAC, that allows to treat targets up to a maximum 120 cm length, the patient must be rotated of 180 degrees during treatment.

The TPS used is able to consider fields with different isocentres in the same optimization process, calculating a single dose distribution and preventing from double dose in junction regions related with misalignment while using overlapping arcs[54]. In such way, dose distribution due to the three dual-arcs planned on HFS-CT was obtained. At this point, critical issue was to optimize the remaining three fields on FFS-CT considering previous dose distribution of the superior part of the body and avoiding double dose in junction region between two CT acquisitions. This was possible, after co-registration of two CT studies, thanks to the "bias-dose" tool of Monaco, that optimizes the cumulative dose distribution while it ensures OAR tolerances and high dose in junction region never exceeded. Treatment plan was performed initially on CT-images of Alderson Rando with legs of bottle to investigate bias-dose properties, but for dosimetry purposes only HFS-plan was optimized because legs of bottles cannot fit dosimeters.

Treatment goals are reported in table 6. Target homogeneity was overcome if near maximum ($D_{2\%}$) and near minimum ($D_{98\%}$) doses were within +10% and -10% of prescription dose (12 Gy), while mean doses to lungs and kidneys (if contoured) should not exceed 10 Gy. These objectives may be modified in the future performing a fine tuning of the protocol.

Structure	Parameter	Treatment goal
PTV$_{12Gy}$	$V_{95\%}$	≥95%
	$D_{2\%}$	<110%
	$D_{98\%}$	>90%
Lungs	D_{mean}	<10 Gy
Kidneys	D_{mean}	<10 Gy

Table 6. Treatment goals of VMAT-based TBI.

2.5 Dosimetric verifications

For dosimetry, two methods were considered. The first one provided for the use of Alderson Rando phantom filled with TLDs, while for the second one, the Delta[4] phantom+ (ScandiDos AB, Sweden), a diodes array phantom, was used. TLDs allowed point measurements while the Delta[4] phantom+ provided dose distributions and gamma-analysis. The most critical issue in this phase was to obtain dose distributions of junction regions between adjacent fields. Usually, Delta[4] acquires beams whose isocentre is centred with respect to the phantom, but to centre the junction regions on diodes planes of the phantom, isocentres of adjacent beams must be shifted. Considering for dosimetry a treatment plan that would be used for treatment of the patients (as described in previous paragraph), irradiation of only two adjacent fields would cover a total length of 76 cm (two adjacent beams of size 40x40 overlapping by 4 cm). However, the phantom has limited sizes (18 cm useful for beam detection) and to avoid damage to electronic part due to its irradiation, the VMAT-TBI plan used for dosimetry consists of four 6 MV x-rays fields of maximum size 40x25 cm^2 planned on four different isocentres spaced 21 cm apart (overlapping region was equal to 4.0 cm as for 40x40 cm^2 fields). In this way irradiation of phantom electronics was avoided. This treatment plan was for dosimetry with Delta[4], but also for Alderson Rando with TLDs measurements, in order to compare results obtained by two methods.

Figure 13. RADOS RE-2000 TLD reader (RadPro International GmbH, Germany).

2.5.1 Dosimetry with Alderson Rando phantom

2.5.1.1 Thermo-luminescent dosimeters and calibration

For dosimetric checks with Alderson Rando, a total of 200 lithium fluoride TLDs of 200GR-A type were used. Before their use, TLDs were prepared by annealing them three times in oven for 25 min at 237°C. Afterwards, prior to each exposure, annealing procedure (25 min at 237°C) was performed once, after each exposure, the TLDs were stored at room temperature for about 24 h prior to read-out. The TLD reading counts were obtained with RADOS RE-2000 TLD reader (RadPro International GmbH, Germany), shown in Fig. 13. The reader is connected to a computer, and its software allows to select its working parameters, like temperature, pre-annealing and reading time. Software collects glow-curves, i.e. counts-temperature/time curves, from which reading counts are obtained. An example of glow-curves obtained from TLD calibration are shown in figure 14; a temperature of 280°C and times of 3.5 sec and 16 sec for pre-annealing and reading, respectively, were selected.
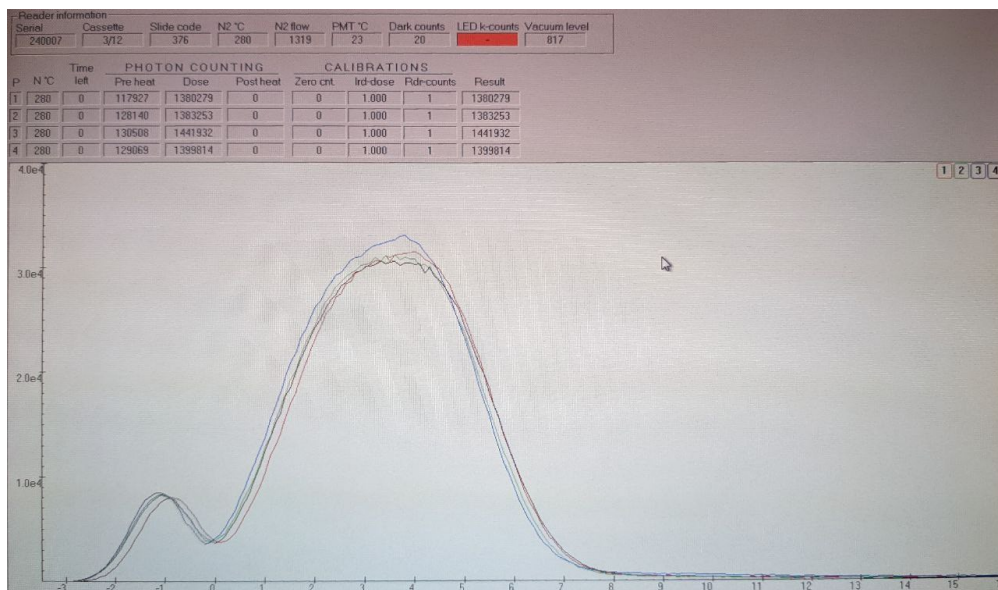

Figure 14. Glow-curves obtained from TLDs reading after calibration exposure.

The calibration procedure was performed to estimate TLDs individual sensitivities by exposing them to a uniform dose of 2 Gy from a 6 MV photon beam under full scatter conditions, with a field size of 20x20 cm^2, SSD of 100 cm, at build-up (1.5 cm) in solid water. To ensure a homogeneous exposure of all TLDs, these were divided into groups of 16 and arranged in the central region of the beam, as shown in figure 15. Moreover, in order to distinguish the TLDs and assign to each of them its own characteristic sensitivity, they were identified with a code, written in pencil on one of their surfaces, consisting of a letter (A, B, C, D, E, H, L, N, S or V) and a number from 1 to 20. Calibration procedure was performed three times, so for each TLD three calibration factors were obtained dividing the known dose by reading counts. Dose was measured with an ionization chamber (0.6 cc farmer type, PTW Freiburg) placed at 10 cm depth in solid water, before irradiating TLDs to obtain the MU necessary to deliver 2 Gy at build-up, and in the meantime that each 16-TLDs group was exposed to radiation to take into account possible beam variations. Individual sensitivities were calculated averaging the three calibration factors and they were used for the future dose measurements with Alderson Rando. For VMAT-based TBI dosimetry, only TLDs that had a response within 5% of the mean of the group and a standard deviation (evaluated by the three calibrations) within 2% were selected, so as to consider only dosimeters with greater response stability. The deviation of response between the various TLDs was not actually important, using specific sensitivities for each dosimeter.
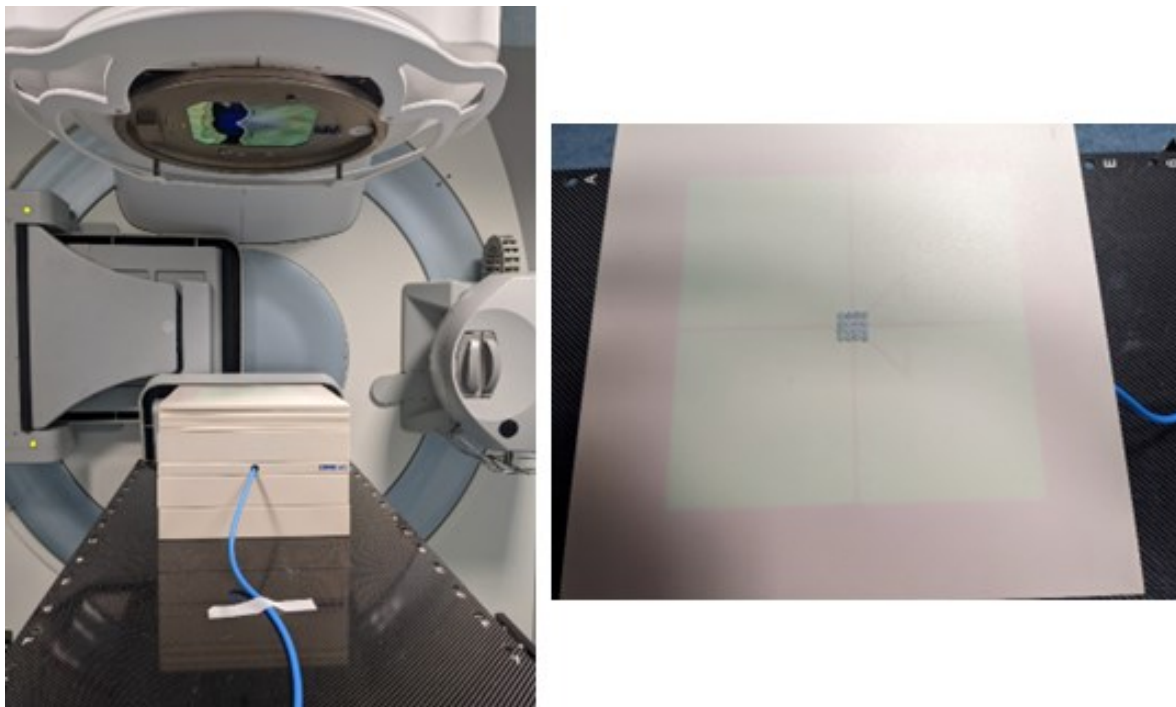

Figure 15. Measurement setup for calibration of TLDs. Phantom made of solid water slices was used. Groups of 16 TLDs were placed in the centre of a 20x20 cm^2 field at build-up (1.5 cm depth) of 6 MV photon beam. Ionization chamber for reference measurements was placed at 10 cm depth, SSD=100 cm.

2.5.1.2 Alderson Rando measurements

After calibration procedure, 114 TLDs were selected and inserted in dedicated holes of Alderson Rando at about half the depth of the slices. In particular, 57 locations were chosen (Fig. 16), spread over 12 slices (4, 5, 8, 9, 12, 13, 16, 17, 20, 21, 24, 25 and 29), those corresponding to positions of isocentres and junction regions of the fields. In each hole two TLDs were positioned, so that they could be seen in CT-scan of 2 mm slices (Fig. 17). The thinnest thickness of the scan (compared to the thickness sufficient in case of a real patient, i.e. 5 mm) is required to be able to see dosimeters, whose thickness is about 1 mm. Being dosimetry possible only on Alderson Rando and not in legs part made of bottle of water, only HFS-CT was required for planning. After CT acquisition, contouring (Fig. 17) and planning were done following indications described above but with four fields of maximum size of 40x25 cm^2, grid spacing 0.2 cm and statistical uncertainty of 0.5% per calculation. Dose was calculated as dose-to-water, being TLDs calibrated in terms oof dose-to-water. Four isocentres were placed on the head, chest, abdomen and the last one on pelvis region, and they were named A, B, C and D, respectively. Three junction regions were obtained and named AB, BC and CD (first letter indicate the cranial field, i.e field that is in cranial direction, while the second letter indicate the caudal filed, i.e field that is in caudal direction). Table 7 reports calculation parameters selected for treatment plan for dosimetric checks with Alderson Rando phantom.
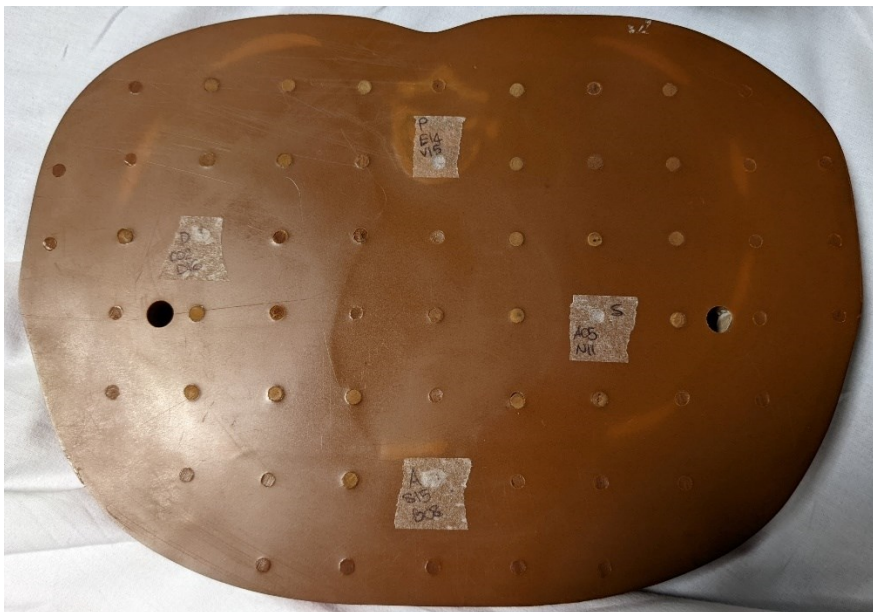

Figure 16. Locations of eight TLDs (two for each location) inserted in a slice of Alderson Rando at about half the depth of the slice.
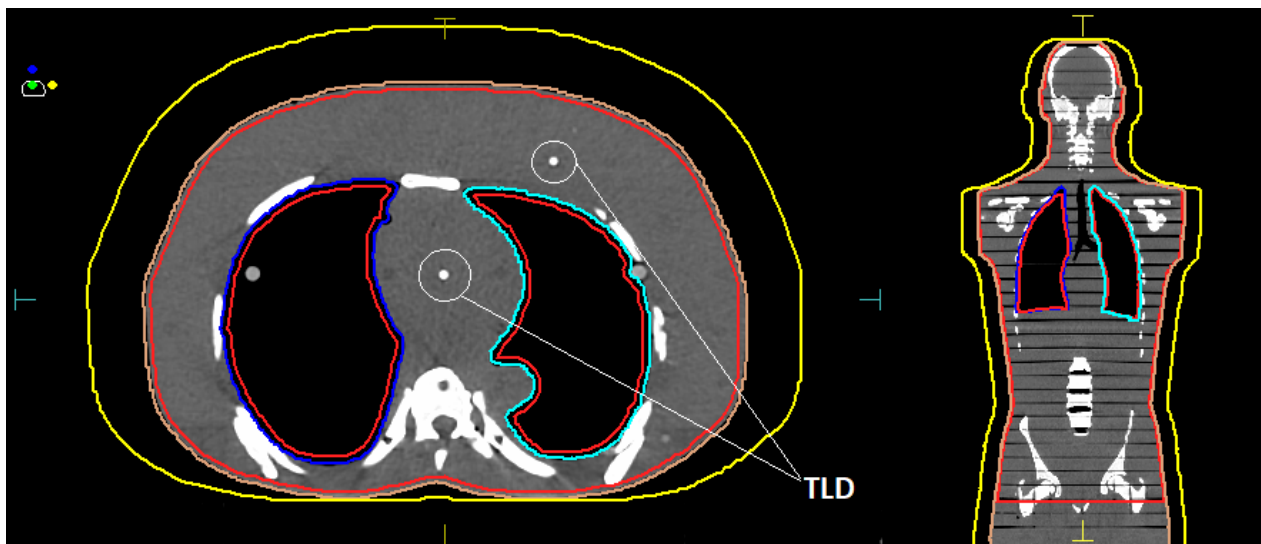
Figure 17. Transversal (left) and coronal (right) views of CT-scan of Alderson Rando phantom. External (yellow), patient (brown), lungs (light and dark blue) and PTV (red) contours are drawn. PTV was obtained contracting patient and lungs contours of 3 mm. TLDs can also be seen circled in the image.

Grid spacing	0.2 cm
Statistical uncertainty	0.5% per calculation
Dose calculation	Dose to water
Minimum segment width	1.0 cm
Fluence smoothing	Medium
Field maximum size	40x25 cm^2
Field increment	30°

Table 7. Calculation parameters of VMAT-TBI plan for dosimetry with Alderson Rando phantom.

After that, Alderson Rando was positioned and aligned with lasers of the LINAC thanks to fiducial markers drawn during the simulation phase (Fig. 18) and VMAT-TBI plan was delivered. Fields took maximum 5 min to be delivered, resulting in an overall treatment time of about 30 min. Being the phantom rigid, no placement verification with CBCT was necessary and positioning was performed based only on the alignment of the markers with the lasers and the longitudinal displacement of the bed between one isocentre and another. Moreover, the use of CBCT would have led to an undue exposure of the dosimeters to radiation not considered in TPS calculation. 16 more TLDs were exposed to 2 Gy at the calibration conditions immediately after the VMAT-TBI delivery to take into account for beam or reader system variations.

After 24 hours, TLD were read with RADOS, following the same reading-procedure used during calibration of dosimeters, to obtain measured dose. Instead, to obtain dose calculated by Monaco, several Volume of Interest (VOI) were created on TLD locations. Interest Points and Markers tool allows to select a point of interest on CT-scan and it creates a sphere volume of desired radius centred on that point. In our case 0.1 cm was chosen due to dimensions of dosimeters (VOI must be contained in TLD volume). After that the VOI was established, statistics with maximum, minimum and mean dose and standard deviation was provided for the 57 points corresponding to TLDs

locations. Calculated dose and its error corresponded to mean dose and standard deviation, respectively, and they were compared to measured dose.

Figure 18. Alderson Rando positioning for VMAT-based TBI delivery.
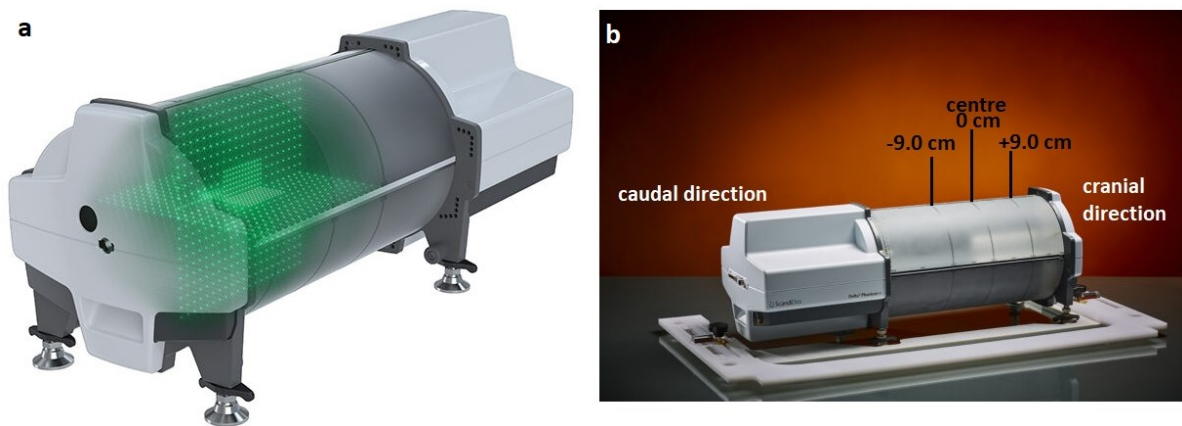
Figure 19. Delta4 phantom+ by ScandiDos AB, Sweden with a) two orthogonal detector planes consisting of 1069 p-type silicon diodes and b) reference system.

2.5.2 Dosimetry with Delta[4]

Dosimetry was performed also with a second method, using Delta[4] phantom+ (ScandiDos AB, Sweden) and the same treatment plan prepared for Alderson Rando measurements. Delta[4] allows to do isocentric measurements in two orthogonal detector planes consisting of 1069 p-type silicon diodes (Fig. 19a). Thanks to wi-fi connection, its software provides instant results: dose distributions on two planes and gamma-index analysis with dose deviation, distance to agreement and gamma pass rate. In order to perform dosimetric checks with Delta[4], dose distribution of VMAT-TBI plan delivered to Alderson Rando was recalculate for each field individually, centred at the centre of Delta[4], in terms of dose-to-water. In this way it was possible to verify the dose delivered by the four

individual beams. However, the most interesting measures were dose distributions in junction regions between fields. This revealed several problems. The first one was due to the limited size of the phantom, only in the central 18 cm the phantom can detect radiation. The second one is to avoid irradiation of electronics, so for this reason VMAT-TBI plan prepared for dosimetric purposes consisted of four fields of 25 cm along longitudinal direction. Third, Delta[4] software can measure cumulative dose distribution of two beams, but these must have isocentres in the same position. In order to place junction regions in the centre of Delta[4], dose distribution was calculated moving the respective caudal isocentre of 9 cm to caudal direction, while the respective cranial isocentre of 12 cm to cranial direction. The first position will be call caudal position and correspond to -9 cm in Delta[4] reference system (0 cm is the centre), while the second will be call cranial position and correspond to +12 cm (see Fig. 19b and 20). If beams were measured at caudal position, they will be call N-CA, while if they were measured at cranial position, they will be call N-CR (N=A, B, C or D). After calculation of the seven plans (four single beams and three coupled beams for junction regions), phantom was positioned on treatment couch and aligned with lasers so that its centre coincided with LINAC isocentre. The four single beams (A, B, C and D) were delivered and dose distributions were measured with the phantom. After these measurements, Delta[4] was moved first by 9 cm in cranial direction, in such way LINAC isocentre coincided with caudal position and the caudal beams (B-CA, C-CA and D-CA) were delivered, then by 21 cm towards the feet, so LINAC isocentre now coincided with cranial position and the cranial beams (A-CR, B-CR, C-CR) were delivered. At this point, however, software of the phantom could calculate dose distributions only if beams were delivered in the same position of the phantom. To overcome this problem, measurements were performed moving Delta[4] as described above, but telling software that beam isocentres were always centred respect to phantom. After acquisition, planned doses were shifted of 9 or 12 cm in appropriate direction so that planned and calculate doses were comparable. Combining A-CR with B-CA, B-CR with C-CA and C-CR with D-CA measurements, dose distributions of the three junction regions were obtained. A total of seven dose distribution measurements (four single beams and three coupled beams for junction regions) were obtained.
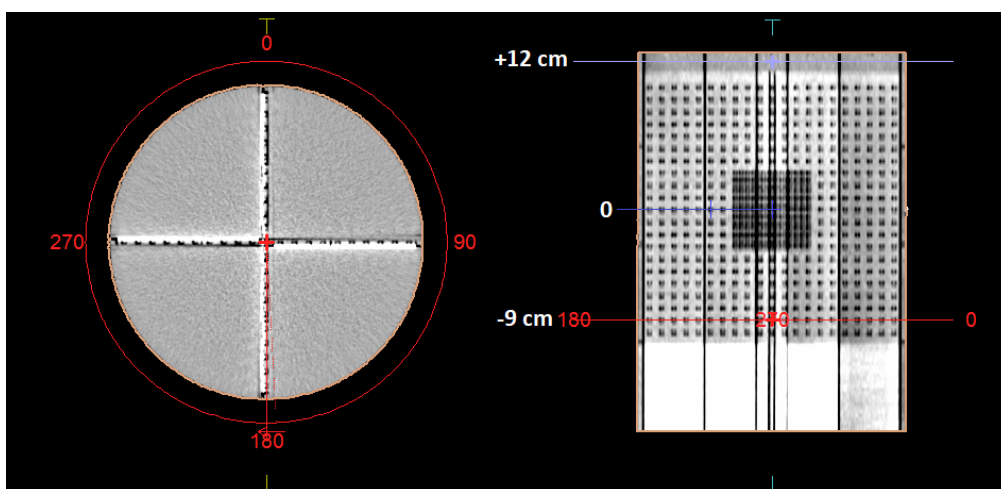
Figure 20. Transversal (left) and coronal (right) planes of CT-scan of Delta[4] phantom+. Two of the four isocentres of VMAT-TBI plan can be observed. One is positioned at -9 cm and the other at +12 cm, so that the junction region results centred respect to the phantom.

2.6 Immobilization systems and position verifications

Immobilization systems and patient's position verifications are treatment aspects which cannot be investigated with a phantom. To identify the best solution to immobilize patient a volunteer's support is needed. Following indications from literature, a thermoplastic mask was proposed to immobilize patient's head and shoulders, while vacuum mattress is used for abdomen and legs immobilization. Immobilization of arms is a critical issue, but the idea is to let patient stretch arms over along body, to fix position with appropriate markers and elastic bands. To verify patient's positioning at treatment unit, CBCT will be performed for each isocentre.

CHAPTER 3
RESULTS

3.1 Alderson Rando treatment plan results

Results of planning with Monaco® 5.51.10 in order to obtain a VMAT-TBI treatment plan are reported in this paragraph. Two measurements with Alderson Rando were performed, so two treatment plans were prepared, one for each measure. Monitor Units and beam-on time for each beam of the plans are reported in table 8, while table 9 shows DVH statistics results, which fulfil treatment goals reported in table 7 (par. 2.4). Dose distribution calculated with Monaco® and DVH of treatment plan prepared for dosimetry with the phantom (Measure 2) are shown in figures 21 and 22, respectively.

Field	Measure 1		Measure 2	
	MU	Beam-on time (min)	MU	Beam-on time (min)
A	533.41	2.75	490.69	2.65
B	1199.75	4.80	1159.37	4.70
C	1182.46	4.75	1110.22	4.55
D	767.91	3.25	718.37	3.10
Overall	3683.53	15.55	3478.65	15.00

Table 8. Monitor Units and beam-on time of two treatment plans planned for dosimetry measurements with Alderson Rando phantom.

Structure	Parameter	Results in phantom	
		Measure 1	Measure 2
PTV$_{12Gy}$	V$_{95\%}$	95.27%	96.13%
	D$_{98\%}$	11.05 Gy	11.15 Gy
	D$_{2\%}$	12.72 Gy	12.73 Gy
Left lung	D$_{mean}$	8.881 Gy	9.067 Gy
Right lung	D$_{mean}$	8.773 Gy	9.034 Gy

Table 9. DVH statistics of treatment plans prepared for Measure 1 and Measure 2 with Alderson Rando and simulations on patients' CT-scans. Prescription was 12 Gy to mean dose of PTV.
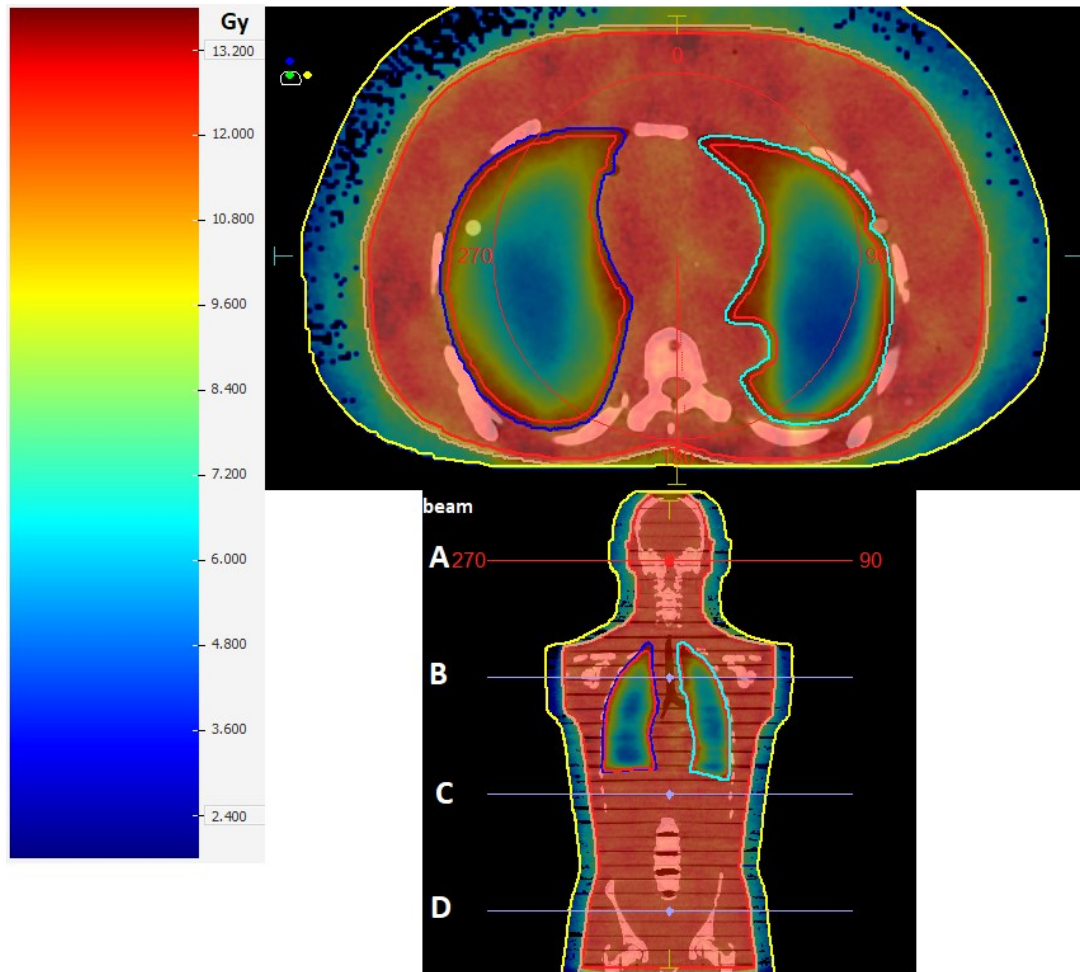
Figure 21. Dose distribution calculated with Monaco 5.51.10® of VMAT-TBI treatment plan prepared for dosimetry with Alderson Rando (Measure 2). In coronal plane, the four isocentres, equispaced by 21 cm, can be observed.
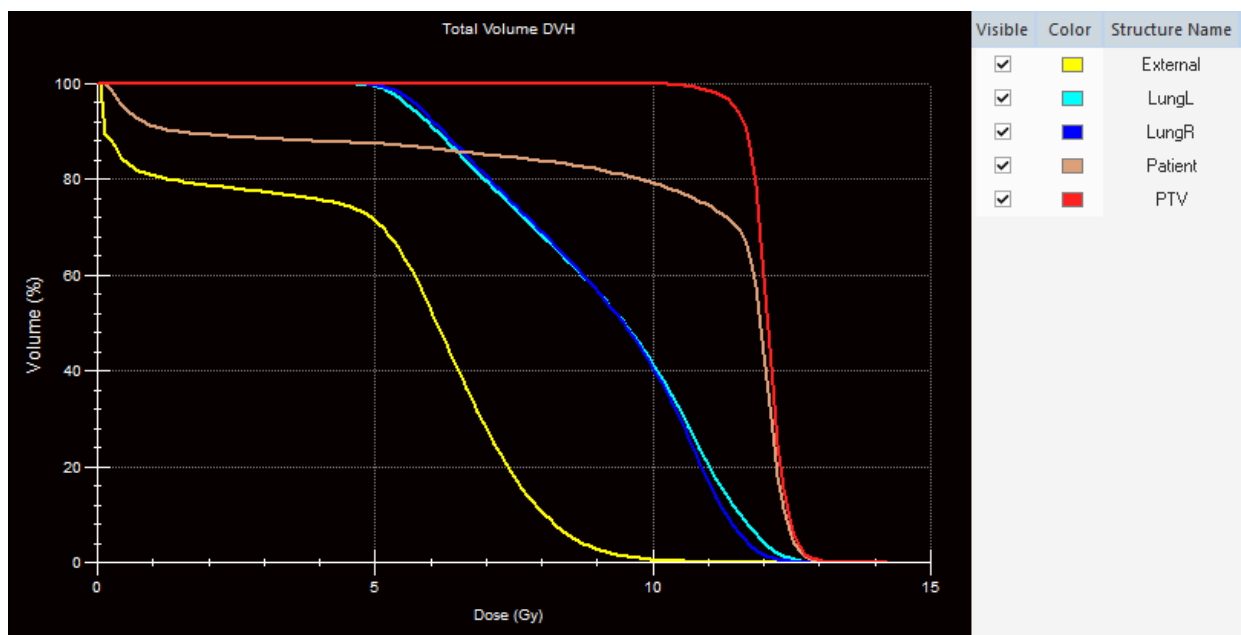

Figure 22. DVH of VMAT-TBI treatment plan prepared for dosimetry with Alderson Rando (Measure 2).

3.2 Measurements with Alderson Rando phantom and thermo-luminescent dosimeters

TLDs were read with RADOS after about 24 hours from irradiation of the phantom. Reading counts of the i-th TLD (C^i) was multiplied by its own sensitivity (S^i) to evaluate measured dose (D_m^i) and eventually by correction factors to take into account LINAC (k_L) and TLD reader (k_r) drifts. Uncertainty of measured dose for i-th TLD (ΔD_m^i) was evaluated with propagating rule, using standard deviation of sensitivity (SD_{S^i}) and poisson statistics for counts uncertainty:

$$D_m^i = C^i \cdot S^i \cdot k_L \cdot k_r$$

$$\Delta D_m^i = \sqrt{(C^i \cdot SD_{S^i} \cdot k_L \cdot k_r)^2 + \left(S^i \cdot \sqrt{C^i} \cdot k_L \cdot k_r\right)^2}$$

For each location in the phantom there were two TLDs, so measured dose is the average of the two measurements, and it was compared with calculated dose that was evaluated as described in previous section as the mean dose of VOI centred on TLD in CT-scan, and its uncertainty was standard deviation provided by TPS.

VMAT-TBI treatment (CT-simulation, planning and irradiation) of Alderson Rando filled with TLDs was performed twice, obtaining two sets (Measure 1 and Measure 2) of 57 measurements. In appendix, results (measured dose by TLDs, D_m, calculated dose by Monaco, D_c, and their uncertainties, ΔD_m and ΔD_c) for the 57 locations of dosimeters inside the phantom are reported in table A1. Percentage dose differences ($\Delta\%$), reported in table A2, between D_m and D_c were calculated as

$$\Delta\% = \frac{D_m - D_c}{D_c}$$

The ranges obtained were -5.7% to 11.5% for Measure 1 and -9.2% to 5.7% for Measure 2. Maximum differences between measured and calculated doses were 11.5% and -9.2%, while the mean differences (in absolute terms) were 2.3% and 2.4% in measure 1 and 2, respectively. Number of points with differences greater than ±5% are 3 for the first set of measure and 7 for the second one (Tab. 10). The greatest differences were found in lungs regions where there was a high dose gradient, that is very influenced by variations occurred in phantom or VOI positioning. Table 11 reports mean percentage dose differences obtained averaging measurements for each slice of the phantom filled with TLDs and for regions distinguished between isocentre regions, where beam isocentres were placed, and junction regions, where adjacent fields overlapped.

The greatest uncertainty in these measurements was due to long-term instability of TLD reader. In first measure, counting readings had a +6% variation respect to calibration, while a -4% was found for the second measure. Thanks to measurements performed with 16 TLDs irradiated in calibration conditions after Alderson Rando irradiation, TLD reader drifts were always taken into account and the adequate correction factors were evaluated and applied to counting readings of TLDs positioned in the phantom.

Results of dosimetry with Alderson Rando and TLDs			
	Measure 1	Measure 2	Average
Max difference	11.5%	9.2%	10.4%
Mean difference	2.3%	2.4%	2.3%
n. of points greater than ±5%	3 (5%)	7 (12%)	5 (9%)

Table 10. Maximum and mean differences between measured (TLDs) and calculated (TPS) doses for 57 TLDs locations and number of points with differences greater than ±5% obtained for Measure 1, Measure 2 and their mean.

Results of dosimetry with Alderson Rando and TLDs					
Region	Phantom slice	Mean Δ% - Measure 1		Mean Δ% - Measure 2	
Isocentre region	4	2.0	1.8	0.6	1.0
	5	1.6		1.5	
Junction region	8	1.5	1.7	3.1	3.1
	9	1.8		3.1	
Isocentre region	12	2.8	3.0	5.5	4.0
	13	3.1		2.5	
Junction region	16	2.2	2.4	4.3	3.3
	17	2.6		2.1	
Isocentre region	20	1.3	1.2	0.5	0.9
	21	1.2		1.3	
Junction region	24	1.9	2.1	1.4	1.7
	25	2.3		1.9	
Isocentre region	29	4.2		2.0	

Table 11. Mean percentage dose differences obtained for each phantom slice that was filled with TLDs and for each region distinguished between isocentre region, where beam isocentres were placed, and junction region, where adjacent fields overlapped.

3.3 Measurements with Delta^4 phantom+

Dose distributions obtained in Measure 2 for single beams centred on Delta^4 phantom+ and for junction regions between adjacent fields are reported in figures 23 and 24. Table 12 reports results for dose deviation (DD), distance to agreement (DTA) and gamma-passing rate (3%/3mm, global, 10% cut) for the seven acquisitions in Measure 1 and Measure 2.
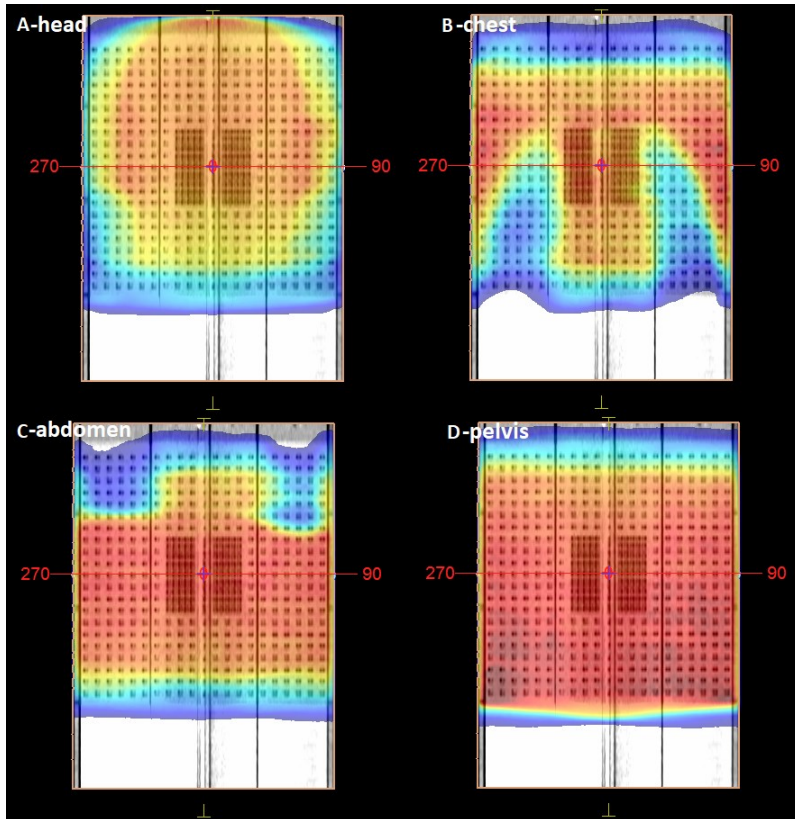
Figure 23. Dose distributions (coronal view) of single beams (A, B, C and D) of VMAT-TBI treatment plan of Alderson Rando calculated on Delta^4 phantom+ with isocentres centred respect to the phantom.
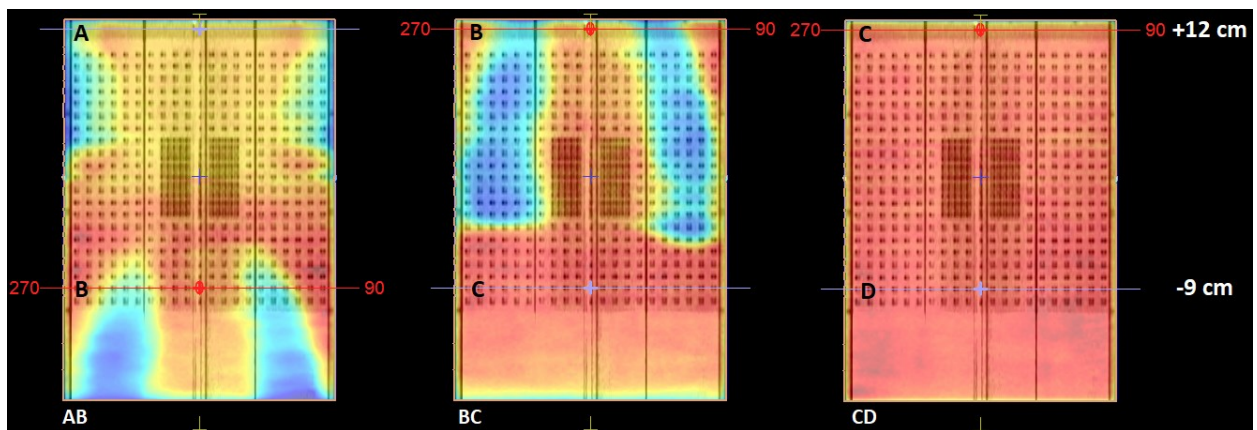

Figure 24. Dose distributions (coronal view) of junction regions (AB, BC, CD) between adjacent fields of VMAT-TBI treatment plan of Alderson Rando calculated on Delta^4 phantom+ with isocentres of beams A, B and C at +12 cm and B, C and D at -9 cm.

Gamma-analysis with Delta[4] Phantom+					
	Measure 1			Measure 2		
Beam	DD (3%)	DTA (3 mm)	γ-passing rate (3%/3mm)	DD (3%)	DTA (3 mm)	γ-passing rate (3%/3mm)
A	99.3%	97.1%	99.9%	97.7%	98.4%	99.5%
B	94.6%	98.2%	99.8%	97.6%	98.1%	99.9%
C	90.5%	91.1%	98.9%	97.6%	96.3%	99.9%
D	97.7%	89.8%	99.7%	97.8%	96.7%	99.4%
AB	77.4%	73.8%	96.2%	83.0%	80.1%	90.8%
BC	60.1%	65.3%	93.6%	59.4%	52.8%	80.7%
CD	69.0%	62.1%	88.9%	72.7%	37.6%	82.1%

Table 12. Results of gamma-analysis for dose distributions of single beams and junction regions between adjacent fields acquired with Delta[4] phantom+. DD = dose deviation, DTA = distance to agreement.

During the analysis a problem due to acquisition of coupled beams was found. When beams A, B, C were acquired at cranial position a greater dose deviation was encountered as shown in figure 25 for beam C. For this beam, the percentage of points that had a dose deviation within 3% passed from 97.6%-96.6%, when the isocentre was positioned at the centre (Fig. 25a) or at caudal position (Fig. 25b), to 70.4% when the isocentre was positioned at cranial position (Fig. 25c), while gamma-passing rate (3%/3 mm) passed from 99.9%-99.7% for measures at the centre or at caudal position to 96% for measure at cranial position. Similar results were observed also for beams A and B in both measure sets. This trend was partly expected observing dose profiles of distributions acquired by two diodes planes of the phantom (Fig. 26 and 27): measured dose is higher than planned dose in caudal direction, so the points with the greatest dose deviation occur in this region. If the beam was delivered with isocentre in cranial position of the phantom the dose distribution was not completely acquired (only the part corresponding to caudal MLC leaves), so the total number of points used for the gamma analysis decreases (from 1069 points for centred beam to 760 for C-CA and 560 for C-CR) and almost all the points with the highest dose deviation are included in the analysis. The result obtained was still acceptable if we considered the limit of 90%, but gamma-passing rate of the coupled beams (C-CR and D-CA to obtain the dose distribution of the junction region CD) did not pass the test (82.1%). To investigate the issue, first of all a shift of 2 mm was applied, considering also dose profiles (Fig. 25d and 27c). Results for coupled beams improved and gamma-passing rate resulted greater than 90% (table 13). However, large variations (higher than 10% in some cases) in DD results between the field acquired at centre or caudal position and the same filed acquired in cranial position were still present. This could suggest a problem with positioning of MLC leaves in caudal direction or with calibration of the phantom, so some extra extended tests were performed. In particular, VMAT plans prepared for LINAC quality assurance were delivered with the same and another Elekta LINAC and acquired with Delta[4] phantom+ in the three positions used for dosimetry of VMAT-TBI treatment (central, caudal and cranial positions). Similar results were obtained in the second LINAC too, excluding a problem with MLC. ScandiDos technical support was requested and it is still helping us to understand the problem due to calibration of the phantom. When Delta[4] acquire a beam, its software applies a correction map, i.e. array of correction factors obtained by phantom calibration performed before its use, to diodes response in order to calculate dose

distribution. The correction map was obtained irradiating the phantom in standard conditions, that is with beams whose isocentre is centred on the phantom. In our case beams had isocentres shifted respect to the centre, so it was supposed that the Delta[4] software is not able to correctly manage correction map shifts with planned dose shifts needed to acquire beams with isocentre in caudal and, in particular, cranial position because the last one was beyond the diodes plate limit.
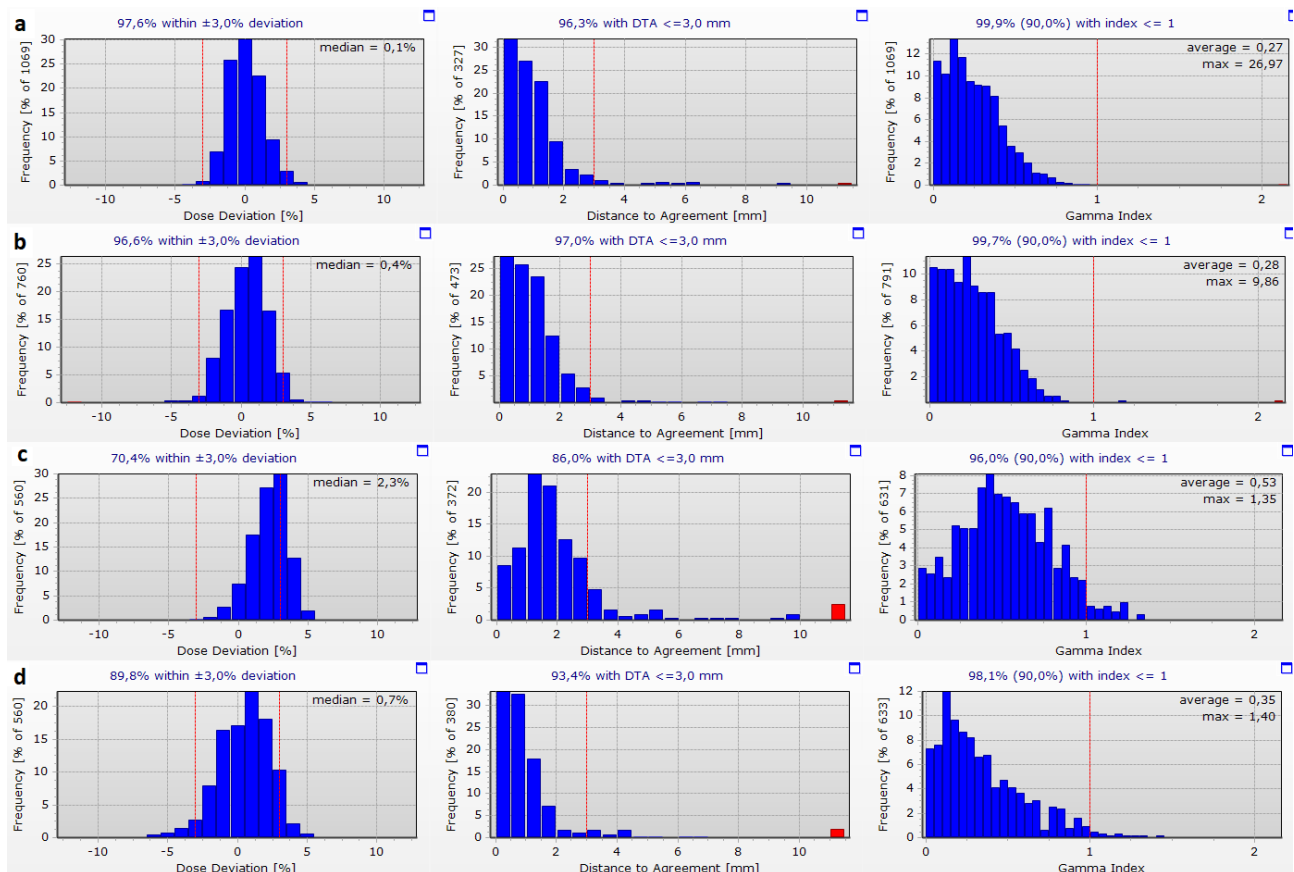
Figure 25. Dose deviation (DD), distance to agreement (DTA) and gamma-index statistics obtained for acquisition of beam C (Measure 2) with Delta[4] phantom+. The beam was acquired (a) centred respect to the phantom (1069 total points), (b) at caudal position (760 total points), (c) at cranial position (560 total points) and (d) at cranial position with a shift of the planned dose of 2 mm.
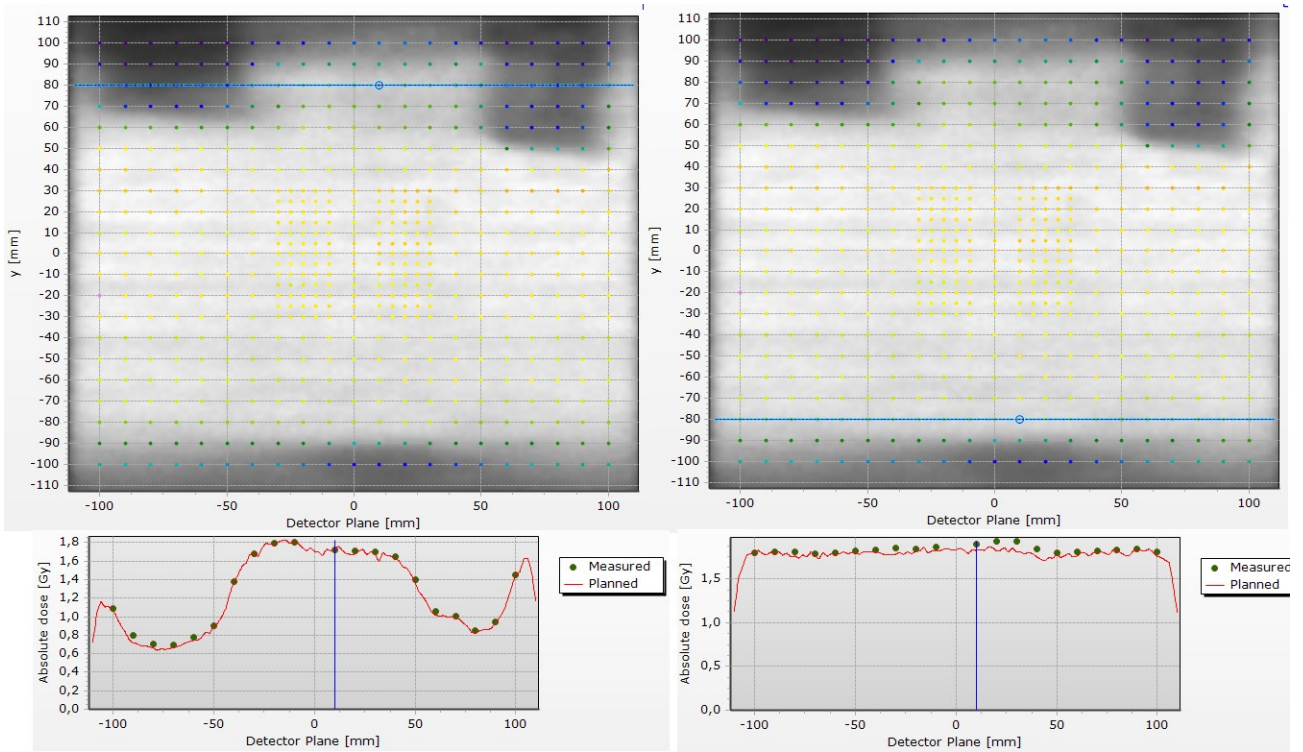
Figure 26. Dose distribution in one of the two diodes array plate and horizontal dose profiles in cranial (left) and caudal (right) direction. Higher deviations between measured and planned dose were found in profile in caudal direction (right).
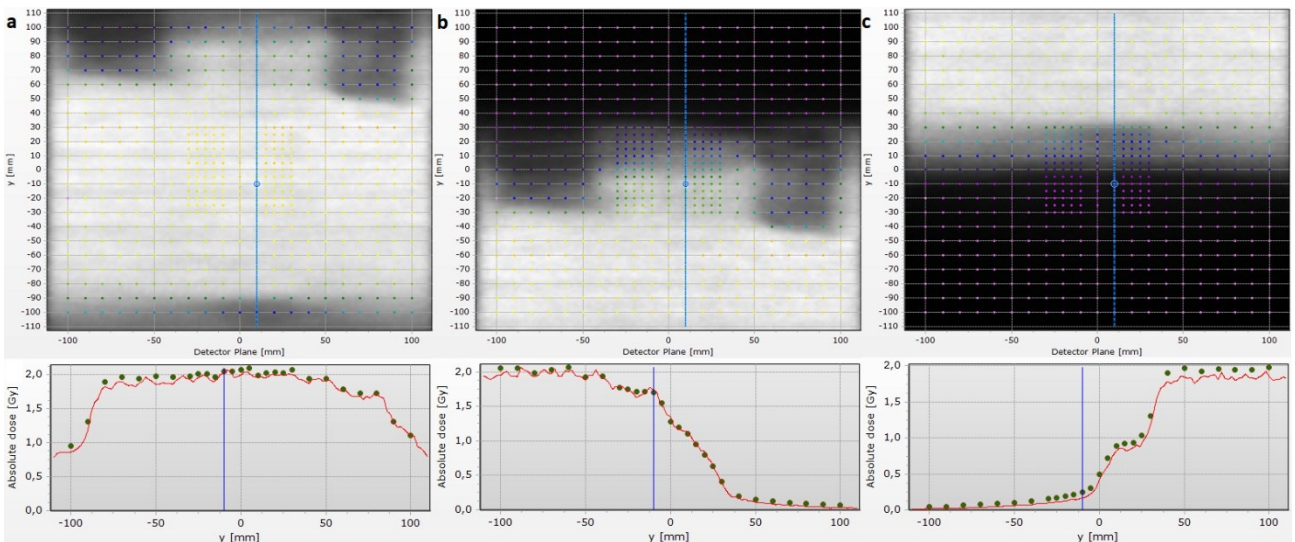
Figure 27. Vertical dose profiles of dose distribution obtained by delivery of beam C with isocentre positioned in the centre of the Delta[4] (a), in caudal position (b) and in cranial position (c). Higher deviations between measured (green dots) and planned dose (red line) were observed in profile of centred beam in caudal direction (negative values of y) and in profile of beam in cranial position, which also shows that a shift of planned dose in -y direction of about 2 mm is needed.

41

Gamma-analysis with Delta[4] Phantom+ - 2 mm shift of planned dose						
	Measure 1			Measure 2		
Beam	DD (3%)	DTA (3 mm)	γ-passing rate (3%/3mm)	DD (3%)	DTA (3 mm)	γ-passing rate (3%/3mm)
AB	83.6%	80.0%	97.1%	93.8%	91.7%	99.2%
BC	73.8%	76.8%	94.2%	77.1%	70.4%	91.0%
CD	78.8%	77.3%	90.8%	87.5%	70.3%	93.5%

Table 13. Results of gamma-analysis for dose distributions of coupled beams in junction regions acquired with Delta[4] phantom+ and after 2 mm shift of planned dose was applied. DD = dose deviation, DTA = distance to agreement.

3.4 Results of patient treatment planning

VMAT-TBI simulated planning was performed for two patients who underwent cTBI treatment and of whom CT-simulation was made as described in paragraph 2.2. Plans on patient's CT-scans consisted of three beams (A, B, C) planned on HFS-scan to irradiate from head to thigh and three beams (D, E, F) on FFS-scan to irradiate from thigh to feet, as described previously. MU are reported in table 14, while treatment plan and DVH statistics are reported in table 15 and figures 28 and 29 for one of the two patients. The results were obtained with both a prescription of 12 Gy to mean dose of PTV and of 12 Gy to cover 90% of the PTV in HFS-scan, as was also suggested by Tas et al (2018)[54]. Prescription for beams planned in FFS-scans were always of 12 Gy to cover 50% of the PTV. Considering treatment goals reported in table 6 (par. 2.4), PTV coverage on HFS-CT plan was fulfilled only with the second prescription, but the near maximum dose ($D_{2\%}$, HFS-scan) of PTV resulted higher than 13.20 Gy (110% isodose) for patient 1. For OARs, mean dose to lungs resulted always lower than 10 Gy, while this did not always happen for kidneys in case of 12 Gy to cover 90% of PTV was prescribed.

MU of VMAT-TBI simulated plan				
	Patient 1		Patient 2	
Beam	12 Gy to mean dose of PTV	12 Gy to cover 90% of PTV	12 Gy to mean dose of PTV	12 Gy to cover 90% of PTV
A	1846.28	1918.10	1855.61	1915.10
B	3043.03	3161.41	2515.40	2596.05
C	1900.15	1974.07	1612.60	1664.31
	12 Gy to cover 50% of PTV			
D	1035.71		1015.21	
E	669.74		695.57	
F	709.74		671.94	

Table 14. MU of the six beams of VMAT-TBI simulated plan for both patients obtained with both prescriptions used in HFS-CT plan (beams A, B and C), i.e. 12 Gy to mean dose of PTV and 12 Gy to cover 90% of PTV, and with prescription of 12 Gy to cover 50% of PTV for FFS-CT plan (beams D, E and F).

DVH statistics of VMAT-TBI simulated plan		Patient 1		Patient 2	
Structure	Parameter	12 Gy to mean dose of PTV	12 Gy to cover 90% of PTV	12 Gy to mean dose of PTV	12 Gy to cover 90% of PTV
PTV$_{12Gy}$ (HFS-CT)	V$_{95\%}$	93.35%	97.36%	94.56%	97.51%
	D$_{98\%}$	10.84 Gy	11.26 Gy	10.95 Gy	11.29 Gy
	D$_{2\%}$	13.05 Gy	13.56 Gy	12.73 Gy	13.14 Gy
PTV$_{12Gy}$ (FFS-CT)	V$_{95\%}$	98.87%		99.34%	
	D$_{98\%}$	11.56 Gy		11.64 Gy	
	D$_{2\%}$	12.61 Gy		12.70 Gy	
Left lung	D$_{mean}$	9.522 Gy	9.89 Gy	9.586 Gy	9.894 Gy
Right lung	D$_{mean}$	9.512 Gy	9.88 Gy	9.601 Gy	9.909 Gy
Left kidney	D$_{mean}$	9.515 Gy	9.89 Gy	9.974 Gy	10.29 Gy
Right kidney	D$_{mean}$	9.676 Gy	10.05 Gy	9.873 Gy	10.19 Gy

Table 15. DVH statistics of VMAT-TBI simulated treatment plans obtained for both patients with prescriptions of 12 Gy to mean dose of PTV and of 12 Gy to cover 90% of the PTV in HFS-CT plan and prescription of 12 Gy to cover 50% of the PTV in FFS-CT plan.
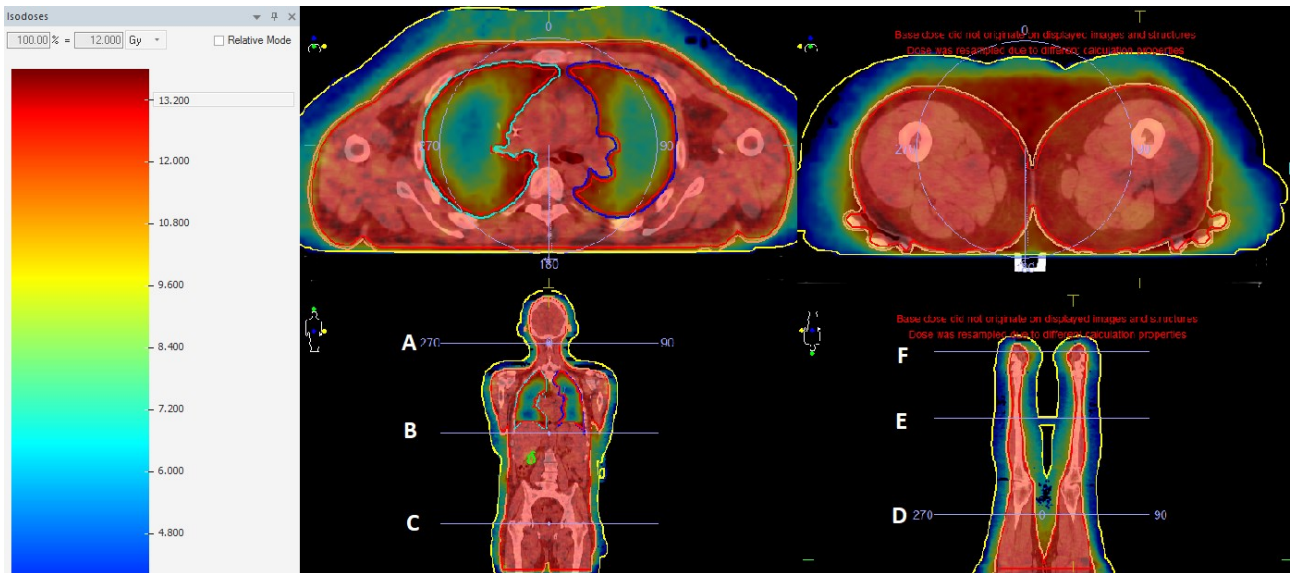
Figure 28. VMAT-TBI simulated treatment plan for one of the two patients (HFS on left, FFS on right) with dose distribution calculated by Monaco 5.51.10®.
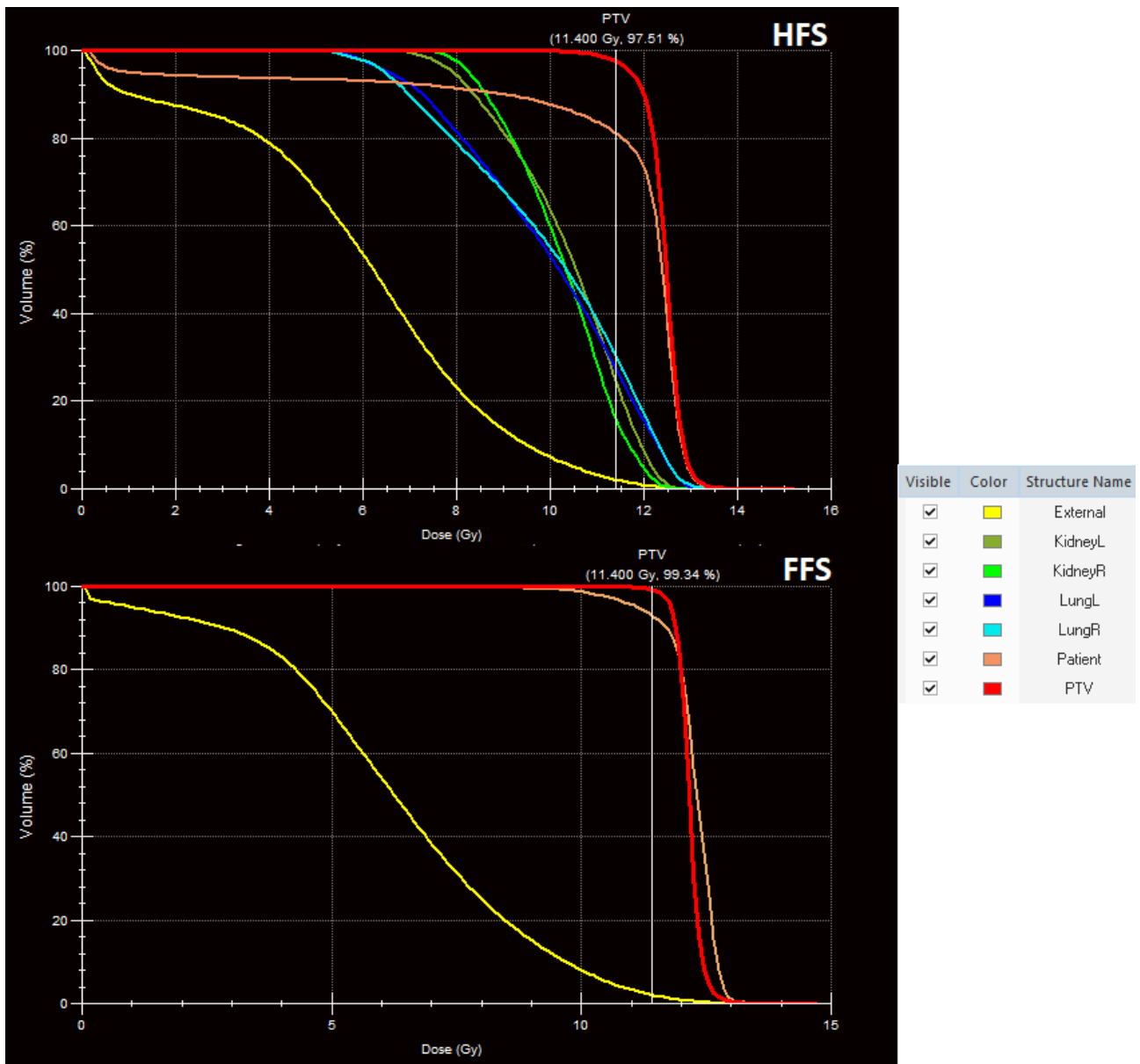
Figure 29. DVHs of VMAT-TBI treatment plan for one of the two patients (HFS on top, FFS on bottom).

The critical issue in planning phase was to optimize beams D, E and F on FFS-CT considering the dose distribution calculated on the other CT-scan. This was important because, as for all the other beams, between the beam C (planned on HFS-CT) and the beam D (planned on FFS-CT) there was a junction region. The dose contribution given by the field C to the VMAT-TBI plan was already calculated and optimized on HFS-CT without considering that another field contributes to dose distribution in the patient, but optimization of the beam D should be performed considering the dose distribution previously optimized. Dose distribution calculated on HFS-CT could be fully integrated on plan optimization on FFS-CT thanks to the Monaco's "Bias" dose tool. Bias dose application on dose optimization can be observed in figure 30: dose distribution given by beams planned on FFS-CT (fig. 30b) is optimized so that it conforms to the one (fig. 30a) already calculated by TPS and given by beams planned on HFS-CT in order to achieve the total dose distribution (fig. 30c) which fulfil constraints imposed by the VMAT planning. Once dose distribution on FFS-CT scan was calculated

44

by TPS with Bias Dose tool, a region of overdoses was observed where the two fields C and D overlapped. This optimization approach was called 3-fields optimization.

Even if clinically accept able, to reduce this overdose, HFS-CT treatment plan (beams A, B and C) was optimized by adding the field D, whose isocentre was positioned at the same coordinates with which it was optimized on FFS-CT, so the optimization was performed on HFS-CT with four beams. Then the field D was deleted from the HFS-CT plan and the optimization of the FFS-CT plan with the Bias Dose was carried out considering the dose distribution of the HFS-CT plan without field D. This approach was called four-filed optimization and it was proposed also by Losert et al (2019)[57]. A comparison of dose distributions obtained with the two approaches is shown in figure 31.
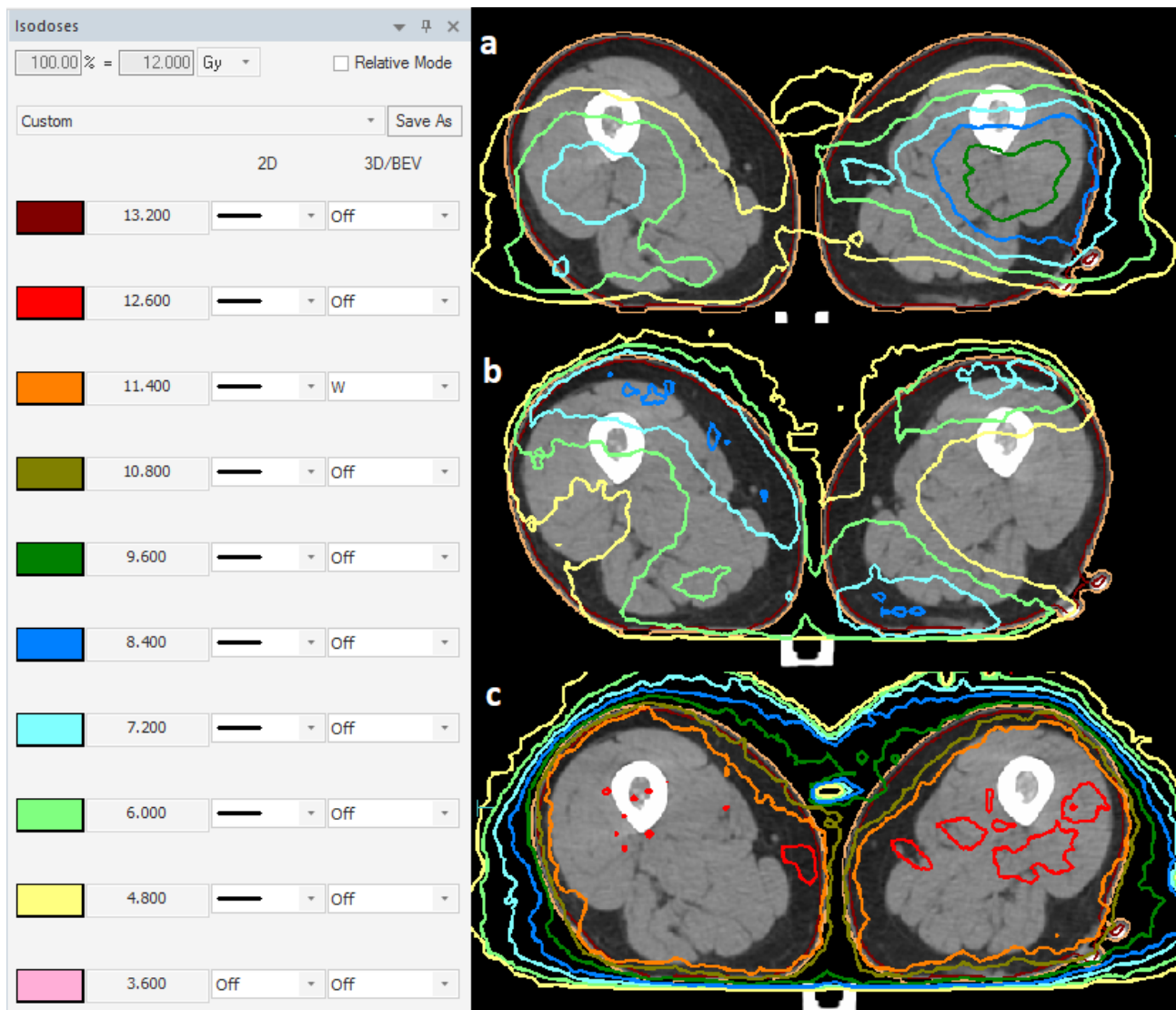
Figure 30. Bias Dose tool application is shown in a slice of the junction region between beams C and D, i.e. the region where HFS-CT plan and FFS-CT plan overlap. (a) Dose distribution optimized previously on HFS-CT plan and given by beams A, B and C is taken into account during the optimization of FFS-CT plan, given by beams D, E and F, so that (b) the resulting dose distribution of FFS-CT plan conforms to the first one in order to obtain a (c) total dose distribution that fulfils VMAT constraints.
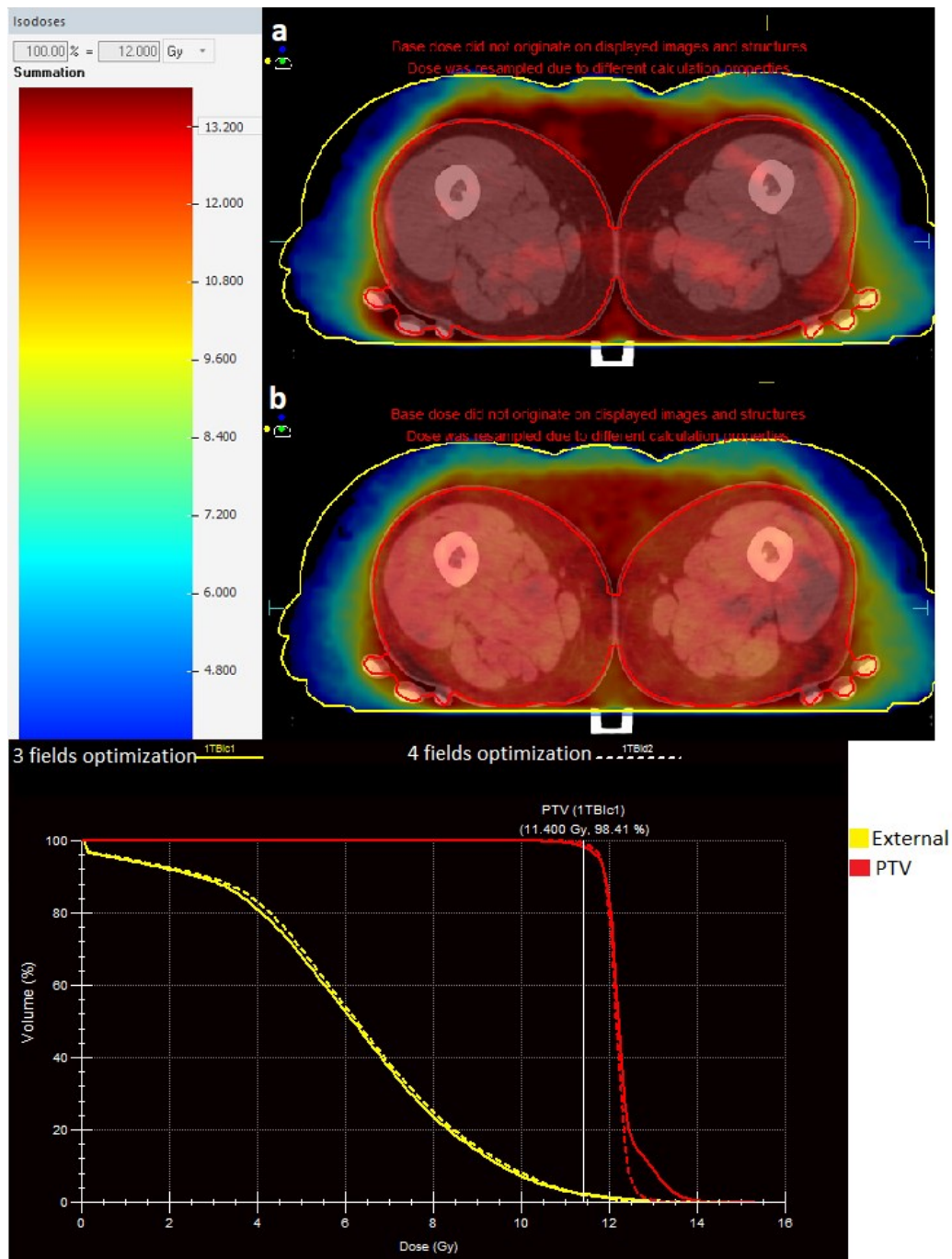
Figure 31. Comparison between the two optimization approaches used is shown in a slice of the junction region where beam C and beam D overlap: (a) optimization of the three beams A, B and C on HFS-CT and then optimization of the three beams D, E and F on FFS-CT with Bias Dose tool, (b) optimization of four beams A, B, C and D on HFS-CT, then elimination of beam D and optimization of the three beams D, E and F on FFS-CT with Bias Dose tool. Overdoses in PTV can be observed on DVH using the 3-fields optimization approach (solid line) compared to 4-fields optimization (dashed line).

CHAPTER 4
DISCUSSION

This feasibility study of VMAT-TBI investigated different aspect of the treatment. First of all, the possibility to perform CT-simulation was verified and two CT-scans, one with head-first orientation and the other with feet-first orientation, can be acquired. In this phase one of the most critical issue are acquisitions of adequate scan length in order to perform correct image fusion and to benefit planning: a greater overlap between the two scans allows a better visualization of the dose distribution in the junction region. HFS-CT/FFS-CT scan length should guarantee to cover the dimensions of the fields that should be planned on HFS-CT/FFS-CT (three in our case for patient's scan) and the first/last isocentre that should be planned on FFS-CT/HFS-CT. In this way, HFS-CT should acquire patient from head to half thigh, while FFS-CT from pelvis to feet, but it should be considered that scan length depends on patient's height. For this reason, the best approach is to acquire an HFS-scout as long as possible (about 150 cm) in order to subsequently adapt CT-scan length to patient's height. Time required for a full CT-simulation was not investigated during the feasibility study because of immobilization systems were not part of this work, but time necessary only for acquisition of two CT-scans (including rotation and repositioning of the patient between one acquisition and the other) was about 30 min.

Contouring can be performed with Monaco® or MIM® and Tas et al (2018)[54] method was adopted. In particular, PTV was contoured with a margin of 3 mm from skin and inside lungs. This choice is in accordance with the current c-TBI performed at GOM Niguarda Hospital, which involves the use of shields for lungs with reduced dimensions compared to the real ones of the organs to assure irradiation of rib cage that is a potential disease site. Therefore, OARs contoured were lungs and, in addition in patient's treatment planning simulation, kidneys. For the dosimetric feasibility study, an in-depth analysis on the contouring aspects is not strictly necessary. These will be discussed with clinicians for next step of implementation, considering that one of the great advantages of this technique is the personalization of the treatment, contouring different specific organs and targets (for example regions that need a radiation boost or higher doses) for each patient. Time required for contouring depends on software that is used (MIM® reduces it from 4-5 hours required using Monaco® to 2-3 hours), organs that have to be contoured and operator experience.

Planning was the treatment phase that took the most time. Calculation time of Monaco® Monte Carlo required about one hour for plan optimization on HFS-CT and about 40 minutes for plan optimization on FFS-CT. To obtain the final optimized plan for VMAT-TBI treatment, it took about 8 hours that will can be reduced with experience and creating dosimetric template inside the TPS. Treatment goals (Tab. 6, par. 2.4) were established considering our current c-TBI and treatment goals prescribed in literature. In particular, for this phase of the treatment implementation more attention was given to PTV coverage and to reduce mean dose to lungs. These are completely fulfilled for Alderson Rando planning with a prescription of 12 Gy to mean dose of PTV. For patient's simulated planning, a prescription of 12 Gy to 90% of the target had to be done to assure coverage of the target in HFS-CT. In this way PTV coverage ($V_{95\%}$) passed from 93.35% with a prescription to mean dose of PTV to 97.36% for one patient and from 94.56% to 97.51% for the other, justifying the

eventual increment of near-maximum dose that exceeded 13.2 Gy (110% isodose). Different studies [53,54,81] performed the same prescription to cover 90% of PTV, taking into account that an under-dosage in this type of treatment could greatly increase the chances of recurrence or relapse. The prescription dose depends on several aspects that consider patient need, so it will be discussed with clinicians for each treatment. Mean dose to lungs is comparable to results obtained in literature, in particular with results of Tas et al. (2018)[55] that used the Elekta TPS and LINAC and the same approach to OARs definitions. Other studies [51,53,56] reach lower doses to lungs but with different definition of the organ, for example contracted of 1 cm from lungs wall. In cTBI performed at GOM Niguarda Hospital, prescribed dose to lungs is equal to 9 Gy. This value is verified with in-vivo dosimetry using diodes which perform point measurements; therefore, it cannot represent a mean dose to lungs that is supposed to be higher, considering that shields have a reduced size compared to those of the lungs (see Fig. 5, paragraph 1.2.1). For kidneys, mean dose resulted higher than goals in case of prescription dose to 90% of PTV, but acceptable for the purposes of the feasibility study considering that in current cTBI performed at GOM Niguarda Hospital kidneys are not shielded and not considered as OARs.

Delivery of VMAT-TBI plan requires about 20 minutes of beam-on time, instead of about 30 min needed for irradiation in cTBI due to low dose-rate set. In our VMAT-TBI technique no restrictions of dose-rate were performed. The mean rates of patient's simulated plans were about 350 MU/min and 200 MU/min for HFS-plan and FFS-plan respectively. However, a maximum limit can be set as a parameter of the treatment and in this case beam-on time increases of about 3 min for each field. Another method to achieve lower dose-rates is the use of treatment plan consisting in four-arc beams, reducing rates to about 200 MU/min. Son et al. (2019)[83] proposed in their work the idea of irradiating only the lung fields with a low dose-rate to keep lung toxicity low while keeping radiation time acceptable if the rest of the fields are irradiated at maximum dose-rate.
The delivery phase consists also of patient positioning. This study could not evaluate the total time required for it, not having yet investigated this aspect. Literature [53,54,57] data assure that the full delivery requires about 1 hour, that is less than the time needed, about 2 and a half hours, for cTBI performed in our centre due to the checks with CR for the positioning of lung shields.

Dosimetry performed with TLDs, our reference for this technique, and Delta[4] allows to verify dose distribution delivered in Alderson Rando and compare to that calculated by Monaco®. In particular, the two measurements with TLDs are comparable between them and with results of the study of Surucu et al. (2011)[2] that used a similar approach for dosimetry obtaining 0.5% and 6.6% for median and maximum percentage dose difference, respectively. In our case higher maximum differences (-9.2%, -8.6% and 11.5%) are observed in lung regions, where there is a greater dose gradient which is influenced more by small misalignments in TLDs positioning. Averaging measurements for different regions, distinguishing isocentre regions from junction regions, it can be observed that mean differences are comparable independently from the type of the region: ranges 1.2%-4.2% and 0.9%-4.0% for isocentre regions, 1.7%-2.4% and 1.7%-3.3% for junction regions in Measure 1 and 2, respectively. This confirms that Monaco plan optimization works properly also for dose calculation in junction regions between adjacent fields.

Several studies [53,54,57] verified the plan robustness to misalignments and this will be one of the next steps of the VMAT-TBI implementation in our centre. In particular, Tas et al. (2018)[54] evaluated the percentage dose differences to mean dose to lungs (range: 2.0%-7.2%), maximum dose to lungs

(range: 2.6%-22.6%) and maximum dose to PTV (range: 3.6%-22.0%) if 3 mm, 6 mm, 9 mm or 12 mm misalignments occurred. CBCT will be introduced for treatment on patients and its effectiveness to reduce misalignments will be studied in the following steps. A qualitative estimate of the setup residual error was performed using Alderson Rando, taking into account that the phantom is inanimate and it cannot represent all possible movements and torsions of a realistic patient. Comparing CT acquisition of Alderson Rando with CBCT images, shift corrections resulted at most 1.8 mm in LAT direction, while lower than 1 mm in the other directions. In order to minimize misalignments of patient's position, the choice of isocentres was made varying only the longitudinal coordinate.

Measurements with Delta^4 confirmed that dose distribution delivered by the LINAC was comparable to that calculated by TPS, accordingly to TLDs results. In particular, all single beams (A, B, C and D) passed the gamma-analysis (3%/3mm) with a percentage greater than 99%, and all coupled beams (AB, BC and CD) with a percentage greater than 90%, after phantom's misalignments corrections. The method proposed for dosimetry with Delta^4 is still in development due to the inappropriate calibration of the Delta^4 when it acquires beams with isocentre shifted from the phantom centre. However, results are supposed to increase once the appropriate calibration will be achieved, and Delta^4 will also be used to verify the dose distribution at the junction region between HFS plan and FSS plan. Similar results with gamma-analysis (3%/3mm) for single beams were found in literature[53,55,74] using different instrumentation for dosimetry, as for example ArcCHECK. This phantom allows to perform dosimetry of junction regions, obtaining a gamma passing rate higher than 95%, but with the use of different TPS and/or LINAC. No studies were found to carry out dosimetry of the junction regions with the Delta^4.

This dosimetric feasibility study has some limitations too, mostly related to instrumentation used for dosimetry. Delta^4 is not properly calibrated for acquisitions of beams not centred respect to the phantom, while TLD reader introduces an uncertainty to measurements due to its long-term instability. This uncertainty can be reduced performing a calibration of all TLDs before each measurement with Alderson Rando and reducing as much as possible the time between calibration and measurement. Moreover, treatment plans prepared for dosimetry do not match exactly the plan that would be used for patient's treatment because it consists of smaller fields (40x25 cm^2 instead of 40x40 cm^2) to avoid irradiation of Delta^4 electronics. However, one of the purposes of the study is to verify if Monaco is able to manage optimization of different beams with different isocentres simultaneously and to calculate the total dose distribution properly. This was verified with two different dosimetric approaches and, due to the fact that fields shape varies during treatment, it was supposed to be independent by fields sizes. Anyway, additional measurements could be performed with the Alderson Rando filled with TLDs and fields up to 40x40 cm^2.

A further extension of this work will be the verifications of plan robustness and the optimization of the patient positioning and immobilization system, including its verification with CBCT implementation on VMAT-TBI treatment workflow.

CONCLUSION

Purpose of this thesis was to investigate the feasibility of TBI treatment for patient undergoing HSCT with VMAT technique in GOM Niguarda Hospital with Elekta Monaco TPS and a Elekta LINAC equipped with Agility MLC. Literature research was carried out to understand evolution of TBI in the past years and new trends, in particular the VMAT technique implementation in other centres. Following the different approaches found in literature, the feasibility study was successfully performed investigating several aspects of the treatment: CT-simulation, contouring, planning and dosimetry.

VMAT-TBI treatment require a whole-body CT-acquisition that is not possible due to couch limitations. However, two CT-scans can be acquired, one with head-first orientation from head to thigh and the other with feet first orientation from thigh to feet. PTV and OARs contouring and then planning can be performed on the two CT-scans, and in particular the dose distributions on two plans can be fully integrated thanks to Bias Dose tool of Monaco. PTV coverage and OARs constraints obtained are increased to those of cTBI, leading a possible benefit to the patient treatment. In particular, it has to be considered that the dosimetric information that we have for cTBI are few and given only by the point measurements of in-vivo dosimetry performed with diodes. Thanks to VMAT technique, clinicians will be able to obtain more accurate dosimetric information from the dose distributions calculated by the TPS. Dosimetry performed with TLDs and Delta^4 confirms that the dose distribution delivered by the LINAC is comparable to that calculated by the TPS, despite instrument limitations.

This study confirms the dosimetric feasibility of TBI treatment with VMAT technique in GOM Niguarda Hospital and its clinical feasibility will be discussed with clinicians. This technique can improve the treatment thanks to its several advantages: a more comfortable patient position, a shorter delivery time, a personalization of the treatment and a well known dose distribution in the patient that can be taken into account to possible new radiation treatments.

APPENDIX

Table A1. Measured dose by TLDs, D_m, calculated dose by Monaco, D_c, and their uncertainties, ΔD_m and ΔD_c obtained for the 57locations of dosimeters inside the Alderson Rando for measure 1 and 2.

Phantom slice	Location	Measure 1 - Gy				Measure 2 - Gy			
		D_m (TLD)	ΔDm	D_c (Monaco)	ΔDc	D_m (TLD)	ΔDm	D_c (Monaco)	ΔDc
SLICE 4	C	2,021	0,007	2,056	0,005	1,957	0,007	1,955	0,005
	A-DX	2,074	0,008	2,084	0,011	1,944	0,009	1,953	0,012
	A-SX	2,014	0,018	2,097	0,011	1,996	0,020	1,967	0,01
	P-DX	2,079	0,021	2,031	0,008	1,980	0,022	1,977	0,006
	P-SX	2,002	0,014	2,029	0,011	1,987	0,016	2,004	0,011
SLICE 5	C	2,123	0,022	2,076	0,014	2,053	0,024	2,043	0,011
	A-DX	2,060	0,017	2,061	0,01	1,981	0,018	2,021	0,022
	A-SX	2,094	0,016	2,059	0,01	2,032	0,017	2,054	0,009
	P-DX	1,978	0,011	2,052	0,009	1,908	0,012	1,971	0,012
	P-SX	2,011	0,013	2,004	0,008	1,994	0,014	1,983	0,009
SLICE8	A	2,105	0,014	2,037	0,014	2,146	0,015	2,04	0,012
	P	2,072	0,012	2,061	0,014	1,979	0,013	1,946	0,019
	DX	2,017	0,021	1,986	0,01	2,054	0,024	1,976	0,005
	SX	2,015	0,015	2,002	0,013	2,078	0,018	2,049	0,011
SLICE 9	C	2,018	0,012	1,996	0,011	1,985	0,013	1,989	0,009
	A	2,130	0,013	2,066	0,009	2,142	0,014	2,026	0,006
	SX	2,042	0,023	2,026	0,012	2,106	0,026	2,027	0,009
	P-DX	2,132	0,022	2,05	0,014	1,988	0,023	2,038	0,005
	A-SX	2,081	0,014	2,082	0,013	2,063	0,015	1,999	0,01
SLICE 12	C	1,955	0,008	2,001	0,012	1,840	0,008	1,964	0,013
	A-DX	2,045	0,020	2,081	0,012	2,012	0,022	2,016	0,007
	A-SX	1,919	0,006	2,035	0,011	1,950	0,007	2,018	0,008
	P-DX LUNG	1,180	0,011	1,201	0,013	1,235	0,013	1,361	0,011
	P-SX LUNG	1,233	0,011	1,264	0,031	1,283	0,013	1,403	0,029
SLICE 13	C	2,019	0,014	2,014	0,013	1,948	0,015	1,963	0,005
	DX LUNG	1,499	0,013	1,345	0,018	1,654	0,017	1,587	0,029
	SX LUNG	1,082	0,007	1,078	0,011	1,112	0,008	1,119	0,015
	A	2,032	0,018	1,977	0,007	2,163	0,021	2,076	0,004
	P	2,088	0,015	2,104	0,031	2,043	0,016	2,096	0,008
SLICE 16	C	2,024	0,016	2,028	0,016	2,066	0,018	1,973	0,008
	A-DX LUNG	1,810	0,016	1,753	0,019	1,923	0,019	1,848	0,014
	A-SX	2,052	0,010	2,08	0,008	2,066	0,011	1,966	0,006
	P-DX LUNG	0,981	0,007	1,008	0,017	1,018	0,009	1,042	0,011
	P-SX LUNG	0,982	0,009	1,017	0,026	1,049	0,011	0,994	0,026
SLICE 17	A	2,037	0,017	2,079	0,014	2,066	0,019	2,011	0,007
	P	2,009	0,022	2,083	0,012	2,155	0,027	2,098	0,015
	DX LUNG	0,866	0,001	0,831	0,004	1,024	0,009	1,001	0,012
	SX LUNG	1,282	0,011	1,275	0,018	1,480	0,014	1,474	0,014

Table A1. (continue) Measured dose by TLDs, D_m, calculated dose by Monaco, D_c, and their uncertainties, ΔD_m and ΔD_c obtained for the 57locations of dosimeters inside the Alderson Rando for measure 1 and 2.

Phantom slice	Location	Measure 1 - Gy				Measure 2 - Gy			
		D_m (TLD)	ΔDm	D_c (Monaco)	ΔDc	D_m (TLD)	ΔDm	D_c (Monaco)	ΔDc
SLICE 20	A	1,997	0,011	2,007	0,006	2,052	0,013	2,043	0,012
	P-DX	1,984	0,013	2,013	0,011	2,021	0,015	2,036	0,018
	P-SX	1,996	0,017	2,032	0,009	2,082	0,020	2,091	0,012
SLICE 21	A-DX	1,945	0,006	1,994	0,008	2,057	0,007	2,042	0,009
	P	2,032	0,023	2,029	0,007	2,077	0,026	2,035	0,009
	A-SX	2,033	0,016	2,056	0,016	2,111	0,019	2,088	0,017
SLICE 24	C	2,050	0,018	2,072	0,007	1,940	0,019	1,985	0,017
	P-SX	1,999	0,016	2,027	0,006	2,001	0,019	2,025	0,009
	A	2,094	0,022	2,054	0,008	2,059	0,024	2,045	0,006
	P-DX	2,012	0,022	2,078	0,013	1,970	0,025	2,001	0,011
SLICE 25	P	2,079	0,021	2,056	0,016	2,013	0,023	2,053	0,008
	C	2,000	0,013	2,098	0,013	1,927	0,014	2,024	0,014
	A-SX	2,041	0,011	2,012	0,005	2,080	0,013	2,077	0,015
	A-DX	2,006	0,014	2,05	0,005	2,021	0,015	2,036	0,008
SLICE 29	C	1,941	0,016	2,052	0,012	1,956	0,017	2,024	0,015
	P-DX	2,008	0,013	2,062	0,010	2,017	0,014	2,033	0,013
	P-SX	1,937	0,011	2,018	0,010	1,961	0,013	1,992	0,006
	A-DX	1,960	0,012	2,054	0,015	1,989	0,013	2,026	0,005
	A-SX	1,914	0,019	2,000	0,008	1,964	0,022	2,010	0,009

Table A2. Percentage difference between D_m and D_c obtained in the two set of measurements with TLDs and their mean for the 57 locations of the dosimeters in the Alderson Rando.

Phantom slice	Location	% difference - measure 1	% difference - measure 2	mean
SLICE 4	C	-1,7	0,1	-0,8
	A-DX	-0,5	-0,5	-0,5
	A-SX	-4,0	1,5	-1,2
	P-DX	2,4	0,1	1,3
	P-SX	-1,3	-0,9	-1,1
SLICE 5	C	2,2	0,5	1,4
	A-DX	0,0	-2,0	-1,0
	A-SX	1,7	-1,1	0,3
	P-DX	-3,6	-3,2	-3,4
	P-SX	0,4	0,6	0,5
SLICE8	A	3,4	5,2	4,3
	P	0,5	1,7	1,1
	DX	1,6	3,9	2,8
	SX	0,7	1,4	1,0
SLICE 9	C	1,1	-0,2	0,5
	A	3,1	5,7	4,4
	SX	0,8	3,9	2,3
	P-DX	4,0	-2,4	0,8
	A-SX	0,0	3,2	1,6
SLICE 12	C	-2,3	-6,3	-4,3
	A-DX	-1,7	-0,2	-1,0
	A-SX	-5,7	-3,4	-4,5
	P-DX LUNG	-1,7	-9,2	-5,5
	P-SX LUNG	-2,4	-8,6	-5,5
SLICE 13	C	0,2	-0,7	-0,3
	DX LUNG	11,5	4,2	7,9
	SX LUNG	0,4	-0,6	-0,1
	A	2,8	4,2	3,5
	P	-0,7	-2,5	-1,6
SLICE 16	C	-0,2	4,7	2,2
	A-DX LUNG	3,3	4,1	3,7
	A-SX	-1,3	5,1	1,9
	P-DX LUNG	-2,7	-2,3	-2,5
	P-SX LUNG	-3,4	5,6	1,1
SLICE 17	A	-2,0	2,8	0,4
	P	-3,5	2,7	-0,4
	DX LUNG	4,2	2,3	3,3
	SX LUNG	0,5	0,4	0,5
SLICE 20	A	-0,5	0,4	0,0
	P-DX	-1,5	-0,7	-1,1
	P-SX	-1,8	-0,4	-1,1
SLICE 21	A-DX	-2,5	0,7	-0,9
	P	0,1	2,1	1,1
	A-SX	-1,1	1,1	0,0

Table A2. (Continue) Percentage difference between D_m and D_c obtained in the two set of measurements with TLDs and their mean for the 57 locations of the dosimeters in the Alderson Rando.

Phantom slice	Location	% difference measure 1	% difference measure 2	mean
SLICE 24	C	-1,1	-2,3	-1,7
	P-SX	-1,4	-1,2	-1,3
	A	2,0	0,7	1,3
	P-DX	-3,2	-1,6	-2,4
SLICE 25	P	1,1	-1,9	-0,4
	C	-4,7	-4,8	-4,7
	A-SX	1,4	0,2	0,8
	A-DX	-2,1	-0,7	-1,4
SLICE 29	C	-5,4	-3,4	-4,4
	P-DX	-2,6	-0,8	-1,7
	P-SX	-4,0	-1,6	-2,8
	A-DX	-4,6	-1,8	-3,2
	A-SX	-4,3	-2,3	-3,3

BIBLIOGRAPHY

1. Wolden, S.L. et al. *American College of Radiology (ACR) and American Society for Radiation Oncology (ASTRO) Practice Guideline for the Performance of Total Body Irradiation (TBI)*. Am J Clin Oncol 36, 97–101 (2013).

2. Surucu, M. et al. *Verification of dose distribution for volumetric modulated arc therapy total marrow irradiation in a humanlike phantom*. Med Phys 39, 281–288 (2012).

3. Cant, A.J. et al. *Practical hematopoietic stem cell transplantation*. Blackwell Pub, 2007.

4. Pasquini, M. & Wang, Z. *Current use and outcome of hematopoietic stem cell transplantation*. CIBMTR Summary Slides (2013).

5. Wong, J.Y.C. et al. *Total Body Irradiation: Guidelines from the International Lymphoma Radiation Oncology Group (ILROG)*. International Journal of Radiation Oncology Biology Physics vol. 101 521–529 (2018). https://doi.org/10.1016/j.ijrobp.2018.04.071

6. Hartman, A.R. et al. *Survival, disease-free survival and adverse effects of conditioning for allogeneic bone marrow transplantation with busulfan/ cyclophosphamide vs total body irradiation: a meta-analysis*. Bone Marrow Transplant 22, 439–443 (1998).

7. Blaise, D. et al. *Long-term follow-up of a randomized trial comparing the combination of cyclophosphamide with total body irradiation or busulfan as conditioning regimen for patients receiving HLA-identical marrow grafts for acute myeloblastic leukemia in first complete remission*. Blood 97, 3669–3971 (2001).

8. Dusenbary, K.E. et al. *Randomized comparison of cyclophosphamide-total body irradiation versus busulfan-cyclophosphamide conditioning in autologous bone marrow transplantation for acute myeloid leukemia*. Int. J. Radiat. Oncol. Biol. Phys. 31, 119–128 (1995).

9. Michel, G. et al. *Allogeneic bone marrow transplantation for children with acute myeloblastic leukemia in first complete remission: impact of conditioning regimen without total-body irradiation--a report from the Société Française de Greffe de Moelle*. Journal of Clinical Oncology 12, 1217–1222 (1994).

10. Bunin, N. et al. *Randomized trial of busulfan vs total body irradiation containing conditioning regimens for children with acute lymphoblastic leukemia: A Pediatric Blood and Marrow Transplant Consortium study*. Bone Marrow Transplant 32, 543–548 (2003).

11. Clift, R.A. et al. *Long-term follow-up of a randomized trial of two irradiation regimens for patients receiving allogeneic marrow transplants during first remission of acute myeloid leukemia*. Blood 92, 1455–1456 (1998).

12. Ringden, L. et al. *A randomized trial comparing busulfan with total body irradiation as conditioning in allogeneic marrow transplant recipients with leukemia: a report from the Nordic Bone Marrow Transplantation Group*. Blood 83, 2723–2730 (1994).

13. Bölling, T. et al. *Retrospective, Monocentric Analysis of Late Effects after Total Body Irradiation (TBI) in adults*. Strahlentherapie und Onkologie 187, 311–315 (2011).

14. Blaise, D. et al. *Allogeneic bone marrow transplantation for acute myeloid leukemia in first remission: a randomized trial of a busulfan-cytoxan versus cytoxan-total body irradiation as preparative regimen: a report from the Group d'Etudes de la Greffe de Moelle Osseuse*. Blood 79, 2578–2582 (1992).

15. Leiper, A.D. *Late effects of total body irradiation*. Arch Dis Child 72, 382–385 (1995).

16. Shank, B. *The balancing act: pneumonitis vs. relapse in cytoreductive regimens containing total body irradiation*. Int. J. Radiat. Oncol. Biol. Phys 36, 261–262 (1996).

17. Ringden, O. et al. *Increased risk of chronic graft-versus-host disease, obstructive bronchiolitis, and alopecia with busulfan versus total body irradiation: long-term results of a randomized trial in allogeneic marrow recipients with leukemia*. Nordic Bone Marrow Transplantation Group. Blood 93, 2196–2201 (1999).

18. Socie, G. et al. *Busulfan plus cyclophosphamide compared with total-body irradiation plus cyclophosphamide before marrow transplantation for myeloid leukemia: long-term follow-up of 4 randomized studies*. Blood 98, 3569–3574 (2001).

19. Della Volpe, A. et al. *Lethal pulmonary complications significantly correlate with individually assessed mean lung dose in patients with hematologic malignancies treated with total body irradiation.* Int. J. Radiat. Oncol. Biol. Phys 52, 483–488 (2002).

20. Hasegawa, W. et al. *Long-term follow-up of secondary malignancies in adults after allogeneic bone marrow transplantation*. Bone Marrow Transplant 35, 51–55 (2005).

21. Curtis, R.E. et al. *Solid Cancers after Bone Marrow Transplantation*. New England Journal of Medicine 336, 897–904 (1997).

22. Thomas, E. et al. *Supralethal whole body irradiation and isologous marrow transplantation in man*. J Clin Invest 38, 1709–1716 (1959).

23. Wong, J.Y.C. & Schultheiss, T. *Radiotherapeutic Principles of Hematopoietic Cell Transplantation*. Thomas' Hematopoietic Cell Transplantation, Fifth Edition. Edited by Forman S.J., Negrin R.S., Antin J.H. and Appelbaum F.R. 22, 244–261 (2016).

24. Girinsky, T. et al. *Prospective randomized comparison of single-dose versus hyperfractionated total-body irradiation in patients with hematologic malignancies*. J Clin Oncol 18, 981–986 (2000).

25. Socié, G. et al. *Influence of the fractionation of total body irradiation on complications and relapse rate for chronic myelogenous leukemia*. Int J Radiat Oncol Biol Phys 20, 397–404 (1991).

26. Thomas, E. et al. *Marrow transplantation for acute nonlymphoblastic leukemic in first remission using fractionated or single-dose irradiation*. Int J Radiat Oncol Biol Phys 817–821 (1982).

27. Deeg, H. et al. *Marrow transplantation for acute nonlymphoblastic leukemia in first remission: toxicity and long-term follow-up of patients conditioned with single dose or fractionated total body irradiation*. Bone Marrow Transplant 151–157 (1986).

28. Ozsahin, M. et al. *Total-body irradiation and cataract incidence: a randomized comparison of two instantaneous dose rates*. Int J Radiat Oncol Biol Phys 28, 343–347 (1994).

29. AAPM Radiation Therapy Committee Task Group 29. *AAPM Report NO.17. The physical aspects of total and half body photon irradiation: a report of Task Group 29, Radiation Therapy Committee,*

Association of Physicists in Medicine. Published for the American Association of Physicists in Medicine by the American Institute of Physics (1986).

30. Bensinger, W.I. *High-dose Preparatory Regimens*. Thomas' Hematopoietic Cell Transplantation, Fifth Edition. Edited by Forman S.J., Negrin R.S., Antin J.H. and Appelbaum F.R. 20, 223–234 (2016).

31. Jacobs, M.L. & Pepe, L. *A total body irradiation chamber and its uses*. Int. J. Appl. Radiat. Isot 9, 141–143 (1960).

32. Sahler, O. D. *Development of a room specifically designed for total body irradiation*. Radiology 72, 266–267 (1959).

33. Leung, P.M.K. et al. *Cobalt-60 therapy unit for large field irradiation*. Int. J. Radiat. Oncol. Biol. Phys 7, 705–712 (1981).

34. Cunningham, J.R. & Wright, D.J. *A simple facility for whole-body irradiation*. Radiology 78, 941–949 (1962).

35. Quast, U. *Physical treatment planning of total body irradiation – Patient translation and beam zone method*. Med. Phys 12, 567–573 (1985).

36. Litoborska, J. et al. *Evolution of treatment planning and dose delivery methods during radiotherapy for patients undergoing bone marrow transplantation: A review*. Nukleonika 65, 19–30 (2020).

37. Malicki, J. *Doses in critical organs during total body irradiation before bone marrow transplantation*. Ann. Transplant 3, 14–19 (1998).

38. Planskoy, B. et al. *Physical aspects of total-body irradiation at the Middlesex Hospital (UCL group of hospitals), London 1988–1993: I. Phantom measurements and planning methods*. Phys. Med. Biol. 41, 2307–2326 (1996).

39. Yao, R. et al. *A simplified technique for delivering total body irradiation (TBI) with improved dose homogeneity*. Med Phys 39, 2239–2248 (2012).

40. Malicki, J. et al. *Cobalt 60 versus 15 MeV photons during total body irradiation: doses in the critical organs and complexity of the procedure*. Ann. Transplant 6, 18–22 (2001).

41. Malicki, J. et al. *The efficacy and reliability of lung protection during total body irradiation of patients with disseminated malignancies*. Neoplasma 52, 325–329 (2005).

42. Kawa-Iwanicka, A. et al. *Dose distribution homogeneity in two TBI techniques—Analysis of 208 irradiated patients conducted in Stanislaw Leszczynski Memorial Hospital, Katowice*. Reports of Practical Oncology & Radiotherapy 17, 367–375 (2012).

43. Giebel, S. et al. *Extreme heterogeneity of myeloablative total body irradiation techniques in clinical practice: A survey of the acute leukemia working party of the european group for blood and marrow transplantation*. Cancer 120, 2760–2765 (2014).

44. Piotrowski, T. et al. *Effect of scattered radiation in the total body irradiation technique: evaluation of the spoiler and wall dose component in the depth dose distribution*. Nukleonika 52, 153–158 (2007).

45. Malicki, J. et al. Total body irradiation before bone marrow transplantation: aims and results. Adv. Exp. Med. Biol. 495, 277–282 (2001).

46. Hui, S. et al. *CT-based analysis of dose homogeneity in total body irradiation using lateral beam*. J Appl Clin Med Phys 5, 71–79 (2004).

47. Hui, S.K. et al. *Feasibility study of helical tomotherapy for total body or total marrow irradiation*. Med Phys 32, 3214–3224 (2005).

48. Zhuang, A. et al. *Dosimetric study and verification of total body irradiation using helical tomotherapy and its comparison to extended SSD technique*. Med Dosim 35, 243–249 (2010).

49. Aydogan, B. et al. *Linac-Based Intensity Modulated Total Marrow Irradiation (IM-TMI)*. Technol Cancer Res Treat 5, 513–519 (2006).

50. Fog, L.S. et al. *A step and shoot intensity modulated technique for total body irradiation*. Tech Innov Patient Support Radiat Oncol 10, 1–7 (2019).

51. Chakraborty, S. et al. *Total Body Irradiation using VMAT (RapidArc): A Planning Study of a novel treatment delivery method*. International Journal of Cancer Therapy and Oncology 3, 03028 (2015).

52. Springer, A. et al. *Total body irradiation with volumetric modulated arc therapy: Dosimetric data and first clinical experience*. Radiation Oncology 11, (2016).

53. Symons, K. et al. *Volumetric modulated arc therapy for total body irradiation: A feasibility study using Pinnacle3 treatment planning system and Elekta Agility^{TM} linac*. J Appl Clin Med Phys 19, 103–110 (2018).

54. Tas, B. et al. *Total-body irradiation using linac-based volumetric modulated arc therapy: Its clinical accuracy, feasibility and reliability*. Radiotherapy and Oncology 129, 527–533 (2018).

55. Uehara, T. et al. *Feasibility study of volumetric modulated arc therapy with Halcyon^{TM} linac for total body irradiation*. Radiation Oncology 16, (2021).

56. Ouyang, L. et al. *Volumetric modulated arc therapy based total body irradiation: Workflow and clinical experience with an indexed rotational immobilization system*. Phys Imaging Radiat Oncol 4, 22–25 (2017).

57. Losert, C. et al. *Novel rotatable tabletop for total-body irradiation using a linac-based VMAT technique*. Radiation Oncology 14, (2019).

58. Zhang-Velten, E.R. et al. *Volumetric Modulated Arc Therapy Enabled Total Body Irradiation (VMAT-TBI): Six-year Clinical Experience and Treatment Outcomes*. Transplant Cell Ther 28, 113.e1-113.e8 (2022).

59. Guo, B. et al. *Image-guided volumetric-modulated arc therapy of total body irradiation: An efficient workflow from simulation to delivery*. J Appl Clin Med Phys 22, 169–177 (2021).

60. Losert, C. et al. *Novel rotatable tabletop for total-body irradiation using a linac-based VMAT technique*. Radiation Oncology 14, (2019).

61. Aristei, C. et al. *Cataracts in patients receiving stem cell transplantation after conditioning with total body irradiation*. Bone Marrow Transplant 26, 503–507 (2002).

62. Belkacemi, Y. et al. *Cataractogenesis after total body irradiation*. Int J Radiat Oncol Biol Phys 35, 53–60 (1996).

63. Bray, L. et al. *Ocular complications of bone marrow transplantation*. Br. J. Ophthalmol 75, 611–614 (1991).

64. Schenken, L. & Hagemann, R. *Time/dose relationships in experimental radiation cataractogenesis*. Radiology 117, 193–198 (1975).

65. Tichelli, A. et al. *Cataract formation after bone marrow transplantation*. Ann. Intern. Med 119, 1175–1180 (1993).

66. Papadimitriou, A. et al. *Growth hormone treatment of growth failure secondary to total body irradition and bone marrow transplantation*. Arch Dis Child 66 (1991).

67. Sanders, E. *Endocrine problems in children after bone marrow transplant for hematologic malignancies. The long-term follow-up team*. Bone Marrow Transplant 8, 2–4 (1991).

68. Thomas, B. et al. *Growth following single fraction and fractionated total body irradiation for bone marrow transplantation*. Eur J Pediatr 152, 888–892 (1993).

69. Carruthers, S. & Wallington, M. *Total body irradiation and pneumonitis risk: A review of outcomes*. Br J Cancer 90, 2080–2084 (2004).

70. Van Dyk, J. et al. *Radiation pneumonitis following large single dose irradiation: A re-evaluation based on absolute dose to lung*. Int J Radiat Oncol Biol Phys 7, 461–467 (1981).

71. Girinsky, T. et al. *Consequences of two different doses to the lungs during a single dose of total body irradiation: Results of a randomized study on 85 patients*. Int J Radiat Oncol Biol Phys 30, 821–824 (1994).

72. Rizzo, J. et al. *Solid cancers after allogeneic hematopoietic cell transplantation*. Blood 113, 1175–1183 (2009).

73. Witherspoon, R. et al. *Secondary cancers after bone marrow transplantation for leukemia or aplastic anemia*. N Engl J Med 321, 784–789 (1989).

74. Morrison, C.T. et al. *Verification of junction dose between VMAT arcs of total body irradiation using a Sun Nuclear ArcCHECK phantom*. J Appl Clin Med Phys 18, 177–182 (2017).

75. Marks, D. et al. *The outcome of full-intensity and reduced-intensity conditioning matched sibling or unrelated donor transplantation in adults with Philadelphia chromosome-negative acute lymphoblastic leukemia in first and second complete remission*. Blood 116, 366–374 (2010).

76. Ringdén, O. et al. *Reduced intensity conditioning compared with myeloablative conditioning using unrelated donor transplants in patients with acute myeloid leukemia*. J Clin Oncol 27, 4570–4577 (2009).

77. Bornhauser, M. et al. *Reduced-intensity conditioning versus standard conditioning before allogeneic haemopoietic cell transplantation in patients with acute myeloid leukaemia in first complete remission: a prospective, open-label randomised phase 3 trial*. Lancet Oncol 13, 1035–1044 (2012).

78. Scott, B. et al. *Myeloablative versus reduced-intensity hematopoietic cell transplantation for acute myeloid leukemia and myelodysplastic syndromes*. J Clin Oncol 35, 1154–1161 (2017).

79. Chen, C. et al. *Radiation-associated pneumonitis following autologous stem cell transplantation: predictive factors, disease characteristics and treatment outcomes*. Bone Marrow Transplant 27, 177–182 (2001).

80. Oertel, M. et al. *Pulmonary toxicity after total body irradiation—an underrated complication? Estimation of risk via normal tissue complication probability calculations and correlation with clinical data.* Cancers 13, 2946 (2021).

81.   Bhatt, C.P. et al. *Elekta Case study Total body irradiation (TBI) using volumetric modulated arc therapy (VMAT)*. https://www.elekta.com/company/medical-affairs/case-study-total-body-irradiation-tbi-using-volumetric-modulated-arc-therapy-vmat/ (2021).

82.   Tas, B. et al. *Dosimetric Evaluation of Total Body Irradiation (TBI) Treatment by Volumetric Modulated Arc Therapy (VMAT) on the coach*. J Biophy Biochem 1, 103 (2017).

83.   Son, J. et al. *Effect of changes in monitor unit rate and energy on dose rate of total marrow irradiation based on Linac volumetric arc therapy*. Radiation Oncology 14, 87 (2019).